

Lipid Biomarker Alterations Following Mild Traumatic Brain Injury

A Thesis
Presented to
The Academic Faculty

By

Eric Christopher Gier

In Partial Fulfillment
of the Requirements for the Degree
Master of Science in Chemistry

Georgia Institute of Technology

May, 2021

Copyright © 2021 by Eric C. Gier

Lipid Biomarker Alterations Following Mild Traumatic Brain Injury

Approved by:

Dr. Facundo M. Fernández, Advisor
School of Chemistry and Biochemistry
Georgia Institute of Technology

Dr. Neha Garg
School of Chemistry and Biochemistry
Georgia Institute of Technology

Dr. Michelle C. LaPlaca
School of Biology
Georgia Institute of Technology

Date Approved: 21 January 2021

Disclaimer: The views expressed in this thesis are those of the author and do not reflect the official policy or position of the United States Air Force, Department of Defense, or the U.S. Government.

DEDICATION

This thesis is dedicated to my mother and father for everything they have done for me over the years. Mom, you have always pushed me to be the best version of myself I could be, and I would not be where I am today without your persistence and dedication to my success. Dad you have been the best role model I could have asked for and I am honored to have had the opportunity to graduate from the Air Force Academy 41 years after you. Coming to Georgia Tech following the USAFA was a dream assignment for me and I have the United States Air Force and the community of people within to thank for that. I have had many amazing opportunities in my life for which I am grateful and will continue to work toward maximizing every one of them.

ACKNOWLEDGEMENTS

I am extremely grateful for all the help and support I have received from Prof. Fernández, Dr. Gaul, and Dr. Alfaro in pursuit of my degree. Prof. Fernández accepted me into his group with open arms and made time for me despite a very busy schedule. Prof. Fernández excels as an instructor and as a mentor and I am fortunate to have gotten to work for him. Dr. Alfaro and Dr. Gaul taught me everything I needed to succeed through this project and answered countless questions along the way. Without their help I would not understand MALDI, LC-MS, and traumatic brain injury to the extent that I do and for that I cannot express my gratitude enough. Without their selfless dedication to my learning, I would not have been able to complete my thesis nor provide the Air Force with the knowledgeable officer it needs.

I would also like to thank the other members of my thesis committee, Dr. Garg and Dr. LaPlaca, for agreeing to take part in my progression as a scientist. Significant time and effort are required of any thesis committee member and they did well beyond anything I could have asked for. Dr. LaPlaca's group, specifically Alexis Pulliam, made this project possible through many hours of hard work. I have enjoyed my time working with her and have no doubt that she has a tremendous career ahead of her.

Finally, I would like to thank the United States Air Force for funding my undergraduate and graduate education thus far. The community of amazing people I have been able to surround myself with because of them has made me into the version of myself I have always wanted to be. I am looking forward to the career ahead of me and everything I will be able to do in service to my country.

TABLE OF CONTENTS

ACKNOWLEDGEMENTS.....	iv
LIST OF TABLES.....	vii
LIST OF FIGURES.....	viii
LIST OF ABBREVIATIONS.....	xi
SUMMARY.....	xiv
CHAPTER 1: INTRODUCTION.....	1
1.1 The Traumatic Brain Injury Epidemic.....	1
1.2 Definitions.....	3
1.3 Modern Clinical Evaluation.....	5
1.4 Injury Mechanisms.....	9
1.5 Laboratory Injury Models.....	11
CHAPTER 2: BIOMARKER STUDIES.....	15
2.1 Biomarker Research.....	15
2.2 Metabolomics Experimental Design.....	19
2.3 Mass Spectrometry.....	21
2.4 Imaging.....	24
2.5 Nuclear Magnetic Resonance.....	25
2.6 Data Workflow.....	26
CHAPTER 3: METHODOLOGY.....	30
3.1 Chemicals.....	30

3.2 Injury Protocol and Blood Collection.....	30
3.3 Serum UHPLC Analysis.....	33
3.5 Data Processing.....	34
3.6 Discriminant Feature Identification.....	36
CHAPTER 4: RESULTS AND DISCUSSION.....	38
4.1 Data Exploration.....	38
4.2 Multivariate Classification Performance.....	41
4.3 Discriminant Metabolite Identification.....	45
4.4 TBI Lipidome Alterations.....	48
4.5 Conclusions.....	50
APPENDIX A: Supporting Information.....	52
REFERENCES.....	62

LIST OF TABLES

Table 1	41
Annotation of lipids in the 5-feature panel discovered in previous research.	
Table 2	46
Annotation of potential candidate TBI biomarkers species in the 16-feature male and 17-feature female optimized panels.	
Table A1	53
Detailed summary of parameters used in genetic algorithms for feature selection.	
Table A2	54
Detailed chemical (MS/MS) fragmentation information of the 23 unique metabolic features that distinguished TBI samples from controls. Ions selected for fragmentation are underlined and ions matched to known and predicted spectra are shown in bold.	
Table A3	61
Permutation test results including sign, Wilcoxon, and Rand's t-test to evaluate model over fitness in male then female sera.	

LIST OF FIGURES

Figure 1	31
<p>Overview of study design, data processing, feature selection and identification. (A) Experimental groups included both the male (n=14) and female (n=18) sexes which were randomly assigned to either sham controls, which received no injuries (n=11), single impact, which received one closed skull CCI injury (n=10), or repeat impact, which received three separate closed skull CCI injuries (n=11). (B) Whole blood was collected at baseline prior to injury and again at 30 min, 4- and 24-h post-injury. (C) Workflow illustrating data collection with LC-MS in both positive and negative ion modes yielding 14,119 features. (D) Peak alignment, picking and integration were accomplished using Compound Discoverer v. 3.0.0, (Thermo Scientific). (E) Following initial feature reduction, 499 statistically significant features of interest with fold changes above 1.5 were identified for further PCA and oPLS-DA modeling. (F) Genetic algorithms were used to create optimized reduced feature panels capable of classifying injured and uninjured serum samples at all collection timepoints. (G) Targeted MS/MS experiments were then performed to identify features present in the final optimized panels. (H) Following identification, biological significance and pathway mapping was undertaken to qualitatively understand features of interest as they relate to mild TBI.</p>	
Figure 2	35
<p>Cloud plot generated in the XCMS web-based application showing positive ion mode retention time versus m/z for features with high fold change and statistical significance between injured (green) and uninjured (red) animals. The black traces outline chromatographic retention time on the x-axis and m/z values on the y-axis for each sample. Each bubble in the plot corresponds to one metabolite feature with fold change at or above 1.5 and a p-value at or below 0.05 using a Welch's t-test. The color and size of each bubble denote the directionality and magnitude of fold change respectively with larger bubbles representing larger fold changes. The darkness of color in each bubble represents p-value significance with darker colors corresponding to features with greater statistical significance. Features with large m/z values are truncated for ease of visibility.</p>	
Figure 3	39
<p>Unsupervised PCA scores plots of the 499-feature list of statistically significant features obtained following filtering and list reduction but prior to final feature panel selection. The distribution of samples shows separation between male and female sexes along the diagonal of PC1 and PC2 explaining a combined total of 45.96% of the variance. Male injured serum is depicted with orange triangles and male uninjured serum is depicted as blue triangles. Female injured serum is shown as pink diamonds and uninjured female serum is shown as green squares.</p>	

Figure 4.....40

(A) oPLS-DA scores plot showing classification by the 5-feature optimized panel derived from previous work differentiating male single impact CCI injuries from uninjured serum samples. (B) oPLS-DA cross validated classification plot using the same 5-feature panel.

Figure 5.....43

(A) oPLS-DA scores plot showing the 16-feature optimized panel to differentiate male injured and uninjured serum samples. (B) oPLS-DA cross validated classification plot using the same 16-feature panel. The panel was used to classify a test set not used during model creation and misclassified no serum samples yielding a Matthew's coefficient of 1.00. (C) oPLS-DA scores plot showing the 17-feature optimized panel to differentiate female injured and uninjured serum samples. (D) oPLS-DA cross validated classification plot using the same 17-feature panel. The panel was also used to classify a test set not used during model creation and misclassified a single 24-hour sample yielding a Matthew's coefficient of 0.83. Permutation tests with 200 iterations were run for both feature panels and further supported a lack of evidence for overfitting.

Figure 6.....45

oPLS-DA scores plot showing the 10-features present in both final panels used to classify injured and uninjured sera at baseline (A) and 30 min (B), 4 h (C), and 24 h (D) post-injury. Sera samples are colored according to injury class where red, yellow, and green sera correspond to repeat injury, single injury, and sham serum samples. An X is drawn at the centroid of each class to indicate average scores on LVs 1 and 2 with the single impact centroids being displayed in black for visibility. Arrows are drawn at each timepoint to indicate centroid movement where the tail of the arrow corresponds to the centroid of the given class at baseline and the head points to the centroid of sera samples at the timepoint of blood collection.

Figure 7.....50

Box plots of selected features from the optimized feature panels to highlight alterations in identified lipid species across blood collection timepoints and sexes. Green and yellow boxplots correspond to male injured and uninjured serum samples respectively and purple and red colored boxplots correspond to uninjured and injured female serum samples, respectively. Black bars within each boxplot are used to show the median normalized area and outliers are drawn as black diamonds. Time point of blood collection is shown chronologically along the x-axis.

Figure A1.....52

Unsupervised Principal Component Analysis score plot of all features prior to feature selection. The distribution of samples shows clustering of quality control samples in the center of all study subject serum samples and separation of reference serum samples from study subject serum.

Figure A2.....53

Cloud plot generated in the XCMS web-based application to portray all significantly differential features from negative mode MS data in injured (green) and uninjured (red) mTBI serum samples. The black traces outline chromatographic retention time on the x-axis and m/z values on the y-axis for each sample. Each bubble in the plot corresponds to one metabolite feature with fold change at or above 1.5 and a p-value at or below 0.05 using a Welch's t-test. The color and size of each bubble denote the directionality and magnitude of fold change respectively with larger bubbles representing larger fold changes. The darkness of color in each bubble represents p-value significance with darker colors corresponding to features with greater statistical significance.

Figure A3.....60

Permutation test results for the male (A) and female (B) optimized panels to evaluate over fitness. Random reordering of class assignments over 200 iterations provided nominally incorrect class assignments to the data and attempted to build models using the same set of features with randomly assigned classes. This method examines the extent to which the models are finding chance correlations between the data and class assignments and overfit to the given data. In general, the cross-validated results shown in blue are relatively close to the self-predicted results shown in green and permuted results shown on the left are far from the un-permuted original model shown on the far right indicating a strong lack of over fitness. The non-permuted results on the far right are more than several standard deviations from the bulk of the corresponding permuted results indicating a lack of over fitting.

LIST OF ABBREVIATIONS

μL	Microliters
μm	Micrometer(s)
ACN	Acetonitrile
BBB	Blood Brain Barrier
CCI	Controlled Cortical Impact
CI	Chemical Ionization
CNS	Central Nervous System
CSF	Cerebral Spinal Fluid
CT	Computed Tomography
CV_m	Coefficient of Variation
Da	Dalton
DDA	Data-Dependent Acquisition
DESI	Desorption Electrospray Ionization
EI	Electron Impact
ESI	Electrospray Ionization
fMRI	Functional Magnetic Resonance Imaging
FT-ICR	Fourier Transform Ion Cyclotron Resonance
g	Gram(s)
GC	Gas Chromatography
GCS	Glasgow Comma Scale
HMDB	Human Metabolome Database
h	hour(s)
HILIC	Hydrophobic Interaction Chromatography
IPA	Isopropyl Alcohol
IS	Internal Standard
LC	Liquid Chromatography

LFP Lateral Fluid Percussion
m/s Meters per Second
m/z Mass to Charge Ratio
MALDI Matrix Assisted LASER Desorption/Ionization
min Minute(s)
mi-RNA micro-Ribonucleic Acid
mm Millimeter
MRI Magnetic Resonance Imaging
MS Mass Spectrometry
MSI Mass Spectrometry Imaging
n Number of Observations
NMR Nuclear Magnetic Resonance
NP Normal Phase
°C Degrees Celsius
oPLS-DA Orthogonal Partial Least Squares Discriminant Analysis
PC Phosphatidylcholines
PCA Principal Component Analysis
PE Phosphatidylethanolamines
PET Positron Emission Tomography
PI Phosphatidylinositols
PL Phospholipid
PLS-DA Partial Least Squares Discriminant Analysis
PLSR Partial Least Squares Regression
PS Phosphatidylserines
QC Quality Control
RP Reverse Phase
s Second(s)
SIMS Secondary Ion Mass Spectrometry

TBI Traumatic Brain Injury

TOF Time-of-Flight

UHPLC Ultra-High Performance Liquid Chromatography

UPLC Ultra Performance Liquid Chromatography

X Data Matrix

Y Class Matrix

SUMMARY

The work presented in this thesis highlights the current state of biomarker research for traumatic brain injury (TBI) and seeks to investigate the potential of novel lipid biomarkers for TBI. Awareness and research interest surrounding TBI have been heightened in recent years due to increased media coverage and epidemics within the military, athletic organizations, accident victims, the elderly, and the general population. The heterogeneous nature of TBI makes diagnosis and biomarker discovery particularly challenging as severities and exposure events vary widely.

The first two chapters serve to outline the current state of TBI regarding its impact on human life, methods of diagnosis, injury mechanisms, and current research in the field. These chapters ultimately highlight a current gap between modern research and clinical implementation that is being closed rapidly through omics research. The final two chapters describe the research conducted over the past year to identify potential lipid biomarkers of TBI. Two predictive lipid panels were developed to classify injured and uninjured Sprague-Dawley rat serum across two injury severities and three acute post-injury timepoints. Identified lipid features from the proposed panels consist primarily of phosphatidylcholine and triacylglyceride species which warrant future investigation as proposed biomarkers of TBI. Ultimately, future work is needed to validate the features identified as potential biomarker candidates and to connect the lipid responses discovered in serum to alterations in the brain lipid profile to gain a more holistic picture of TBI.

CHAPTER 1

INTRODUCTION

1.1 The Traumatic Brain Injury Epidemic

TBI is the result of a direct or indirect blow to the head which disrupts normal brain function. Today, TBI is commonly referred to as the silent epidemic because of its large contributions to the global death toll and disability rate, while still managing to go unreported or misdiagnosed in many cases. Diagnosing TBI is highly subjective in the modern clinical setting and individuals often do not pursue medical attention unless symptoms are severe. Despite this, public awareness has heightened in recent years particularly due to an increase in media coverage of Iraq and Afghanistan war veterans returning home with significant head injuries. Military personnel, athletes, children, and the elderly are among the groups most at risk for suffering a TBI event and public attention surrounding these groups and others has fueled the need for objective testing and treatment options, which are currently lacking.^{1,2,3}

The greatest challenge in understanding TBI lies within its heterogeneous expression among individuals. Factors such as age, sex, and previous exposure to TBI can all impact the way symptoms present themselves.^{4,5} Heterogeneity and injury type are thought to be major factors in the high failure rates of clinical drug trials in the acute phase of injury where neuroprotection is paramount.⁶ Statistics from industrialized countries estimate TBI to occur in between 1 and 26 people per every 2,000, with the greatest rates of incidence occurring in Europe and the United States.^{7,8} Incidence rates in less developed countries are much harder to gauge as reporting methods and hospital

admission criteria differ vastly, however high TBI incidence rates are unlikely unique to the industrialized world.^{9,7}

In 2014, the Center for Disease Control (CDC) reported approximately 2.87 million TBI-related hospitalizations, emergency room visits, and deaths in the United States.¹⁰ Data from the previous eight years, dating back to 2006, showed an increase of deaths by 6% as well as an alarming 54% increase in emergency department visits across the country. Hospitalization rates for the elderly, those 75 years and older, as well as children under the age of 10 are among the highest of all age groups. This is particularly concerning given the increased likelihood of negative outcomes following TBI in old age and the potential for irreparable brain damage during crucial development stages for small children.¹¹

Approximately 80% of all documented TBI cases are considered mild, totaling approximately 1.2 million cases annually in the United States alone.^{8,12,13} These estimates are likely much lower than true incidence rates as many mild TBI cases go misdiagnosed, unreported or undetected in modern health care systems.^{14,15} Symptoms of mild TBI commonly include, but are not limited to, dizziness, loss of concentration, fatigue and loss of memory.^{16,17} While most patients see declining symptoms within 3 months, many report persisting symptoms well beyond, which can significantly impact quality of life. In addition to symptoms, survivors of severe TBI often incur an economic burden exceeding \$600,000 over the lifetime of their injury.¹⁸ Considering the costs of treatment, loss of worker productivity, and death, the United States experiences an estimated \$9 billion in annual expenses as a result of TBI.¹⁹

1.2 Definitions

The major categories of brain injury are defined based on the integrity of the skull. Open TBI, commonly referred to as penetrating skull injuries, result when there is a fracture, break or penetration of the skull. This type of injury commonly occurs in the presence of high velocity loose debris or bullets that penetrate the skull and damage underlying regions of the brain along which the object traveled.²⁰ Closed TBI is far more common in the general population and results from an outside force impacting the brain without breaking the skull.^{21,22} These types of injuries commonly occur during sporting events, in the presence of powerful shockwaves, after a fall, or following head impact with a vehicle after a crash. Symptoms of both categories of TBI vary depending on the regions of the brain that are damaged and the severity of the impact.

Another method of classifying brain injury relies on when damage occurs relative to the time of initial impact. Primary brain damage occurs during or immediately following an impact and can result in skull fracture, contusions (brain bruising), brain bleeding, nerve damage and laceration.²³ Primary damage to the brain can occur directly at the site of impact (coup) as well as to the opposite side of the brain (countercoup) when the impacting force is powerful enough to move the brain inside the skull and cause additional collisions.²⁴ Secondary damage is initiated at the moment of injury, but clinical presentation is delayed; secondary injury mechanisms often include hypoxia where regions of the brain are starved of oxygen, edemas or brain swelling, hematomas, and death of brain tissue.^{23,25} Primary and secondary injury mechanisms both play a role in the heterogeneity of TBI and vary significantly between individuals and injury events.

The relative size of an injury is commonly referred to as either focal or diffuse.

Focal injuries describe damage that is localized to a small region of the head leading to damage at or near the initial injury site. Focal injuries are commonly mimicked in a laboratory setting using controlled cortical impact (CCI) or lateral fluid percussion (LFP) methods.^{26,27} Diffuse injuries occur when a large area of the brain is damaged and are commonly caused by acceleration and deceleration of the brain inside the skull and typically result in axonal injury.²⁸ Laboratory methods for studying diffuse injuries are less commonly employed than focal injury methods but often include LFP, weight drops, or shock tubes filled with compressed gas.²⁹

Injury severity is commonly classified on a scale ranging from mild to severe, and in a clinical setting depends largely on symptom reporting, physician monitoring and structural imaging modalities, when required.³⁰ Mild severity injuries are diagnosed when the patient shows little or no loss of consciousness, alteration in mental state, or amnesia and no signs of abnormality in structural imaging. Moderate injuries are defined by either loss of consciousness for longer than 30-min but shorter than 24- to 96-h, amnesia lasting between 3-h and 1 week, alteration of mental state for greater than 24-h, or abnormal structural imaging results.^{31,32} Severe TBIs are diagnosed when the patient suffers loss of consciousness for longer than 24-h, amnesia for greater than 7 days and has abnormal structural imaging results.³¹ Glasgow comma scale results within the first 24-h of injury are also commonly used in conjunction with other methods in the clinical setting to diagnosis TBI severity.

1.3 Modern Clinical Evaluation

The Glasgow Comma Scale (GCS), originally presented in 1974, holds relatively widespread acceptance in the medical community and is commonly used to assess a patient's motor, verbal, and eye-opening responses after TBI.³³ Patients evaluated with the GCS are graded on a scale of 3-15 with lower scores corresponding to higher injury severity. The scale is divided into three sections with 4 points measuring eye-opening ability, 5 points measuring verbal response and 6 points measuring motor skills. Patients scoring between 13-15 points are considered to have suffered mild injuries and comprise approximately 80% of all TBI cases.⁷ Moderate injuries range from 9-12 and are a large point of contention for the usage of the GCS due to unreliable monitoring of consciousness and inconsistent predicting of outcomes for patients in this range.³⁴ Severe TBI is diagnosed when a patient scores 8 points or fewer and corresponds to significant impairment in at least two areas of the GCS and often requires surgical intervention.³⁵ While the CGS is designed to maximize objectivity in a largely subjective situation many confounding factors such as the presence of brain inhibiting substances, inability of a patient to open their eyes for reasons other than brain injury, and lack of evaluation prior to injury hinder its ability to make accurate assessments in all cases.^{36,37,34}

Another point of contention surrounding the GCS is its failure to include brainstem reflexes in its evaluation.^{38,39} This has led to the development of many other brain injury evaluation scales that are often more complex than the GCS. One example is the Comprehensive Level of Consciousness Scale which includes all the components of the GCS but also evaluates posture, abnormal ocular movements, eye position, pupillary light reflexes, and general responsiveness.⁴⁰ The advantage of this type of scale lies in its

wider range of scores that are better able to capture more subtle differences in a patient's symptoms. While other scales may prove advantageous in describing TBI over the GCS, especially in moderate TBI instances, they are much less widely utilized, require more work from physicians, and still suffer from similar disadvantages in objectivity that may be overcome by more analytical methods.

Loss of static and dynamic balance are among the most reported symptoms following TBI and have been evaluated extensively to monitor patient recovery. Balance deficits are often measured using variations of the Romberg test, tests of postural sway, and the Berg Balance Scale.^{41,42,43,44,45} While balance issues tend to resolve themselves over time, long-term and permanent cases of anterior-posterior and medial-lateral posture issues are common.⁴⁶ Low technology balance assessments offer a quick and cost-effective way of measuring a person's balance and have become popular in many athletic programs for their ability to be performed quickly on the sidelines. One well known example is the Balance Error Scoring System which uses only foam and a stopwatch to evaluate injured athletes. In this assessment, injured persons are asked to perform a series of balance tests first on both and then on individual legs, from both stable ground and on a piece of foam.^{47,48} A major advantage of this method is that baseline tests are performed at the beginning of a long event such as an athlete's season for comparison after injury. Like the GCS, balance assessments lack complete objectivity, which is of particular concern when coaches or athletes want to continue a season despite injuries. These methods have also been criticized as potentially being influenced by player fatigue and injuries unrelated to the brain.⁴⁹

Other less commonly used low technology assessments include dual-task testing,

virtual reality, and gait assessment testing. Dual-task methods require the participant to answer thought questions while simultaneously performing balance testing. These tests are often used in conjunction with regular balance testing to ensure a TBI patient's quality of life when performing daily tasks which require simultaneous cognitive and physical demands.^{50,51} Virtual reality testing, while uncommon in practice due to expense, requires participants to be exposed to images of moving rooms or other dynamic and demanding visual scenes while performing balancing tasks. When available these methods offer a unique opportunity to simulate real life events such as cooking in a kitchen and can be used to monitor injury recovery.^{52,53} Gait assessment testing can be done singularly or in a dual task manner and measures the participants posture and balance while walking or while walking and solving basic mental tasks.⁵⁴ Gait stability especially in a dual-task manner is particularly sensitive to long-term disruptions after TBI and is thought to be well suited for detecting pathological behavior changes.^{55,56} Low technology testing done in a dual-task manner generally shows greater similarity to high technology methods for diagnosing concussion severity than do low technology methods done in isolation. Low technology methods have the advantage of being rapidly deployable, inexpensive, and minimally reliant on self-reported symptoms however, these methods are often biased by observers, and lack necessary biological evaluation.

Modern imaging techniques are the most common form of high technology assessments used in clinical evaluation of TBI and are primarily used to determine the need for surgical intervention or to identify optimal non-surgical treatment options. Neuroimaging also provides a minimally invasive way to monitor injury progression and proves useful in certain cases for detecting the onset of complications that arise long after

injury. Computed tomography (CT) is the most widely used neuroimaging technique during the acute phase of injury for detecting hemorrhages, skull fractures, and parenchymal injury.⁵⁷ The technique works using narrow X-ray beams which travel through the cranium at exact angles and is more cost effective than most other common imaging modalities. CT is especially useful in identifying bone fragments and foreign object debris in the brain making them ideal for understanding unique open skull injuries.⁵⁸

Positron emission tomography (PET) is used to detect changes in metabolic rate and requires the use of a radioactive tracer which accumulates in tissue regions consuming large amounts of glucose.⁵⁹ Studies using PET on TBI subjects have shown the brain's metabolic rate to be highly time dependent. Glucose consumption generally increases in the hours following injury but falls off dramatically by the 24 h timepoint in mild injuries.⁶⁰ Similar studies of severe injuries have reported increased glucose consumption as far as 8- and 10-days post-injury.⁶¹ PET scans are less commonly used to evaluate TBI because of their high cost and low spatial resolution compared to magnetic resonance imaging (MRI), but are useful in cases when limiting patient motion is problematic.

Functional MRI (fMRI) techniques detect changes in vascular activity by taking advantage of the rising oxygen demand resulting from increased neuronal activity. Release of oxygen from red blood cells converts oxyhemoglobin to deoxyhemoglobin and differences in magnetic properties between these forms of hemoglobin are detectable with contrast imaging.⁶² fMRI poses virtually no risk to patients and is fully non-invasive but is highly sensitive to patient motion during scanning and cannot be used on patients

with metal implants.⁶⁰ Studies using fMRI on TBI patients have implicated a link between memory deficit and medial temporal lobe dysfunction as well as differences in activation of the bilateral and prefrontal cortexes with increasing working memory load.^{63,64} The majority of mild TBI cases including symptomatic and asymptomatic patients exhibit normal CT, PET, and MRI scans which leaves a large need for specific diagnostic methods capable of detecting minor differences in brain pathophysiology present in mild injuries.⁵⁹

1.4 Injury Mechanisms

TBI is a multifaceted neurological problem, beginning with immediate and irreversible primary damage followed by numerous and complex secondary injury cascades. The type, focal or diffuse, and severity of primary injury, determine the extent of secondary injury. Primary injury is best managed through preventative measures for example by wearing personal protective equipment, however in the hours and weeks following initial insult, secondary cascades control the extent of damage to the brain.⁶⁵ Mitigating secondary injury cascades represents a major goal in fighting the progression of TBI because of the window of time that exists for clinical intervention. Treatment measures are, however, significantly challenged by the host of diverse TBI etiologies.

Primary injuries occur within a short span, approximately 100 milliseconds, following injury but can severely damage cranial subsystems and shear blood vessels inside the brain. The onset of TBI is often plagued with tissue damage, inhibited cerebral blood flow, and hindered metabolic processes. The orbitofrontal and anterior temporal lobes are among the most affected regions of the brain during primary injury due to their

proximity to the irregular surface of the skull however, cell loss and neuronal damage are also commonly reported in the cerebral cortex, hippocampus, and thalamus.^{66,67,68} Lack of oxygen and blood flow in the brain lead to increased anaerobic glycolysis, the accumulation of lactic acid, depletion of ATP, and the ultimate failure of energy dependent ion pumps which regulate cells. The physiological response to TBI often yields significant hypertension of arteries which is theorized to initiate arachidonic acid cascade events that lead to the downstream formation of free radical species.⁶⁹

Well known secondary injury mechanisms contribute to cell loss, axonal injury and synaptic dysfunction which cause the cognitive impairment that follows TBI. Secondary injury events are prolonged and are often the deciding factor in a patient's survival. Mechanical damage from the primary injury and membrane depolarization from injury induced ionic imbalances result in a large release of excitotoxins like aspartate and glutamate into the extracellular space. The influx of these excitotoxins leads to membrane depolarization and activation of excitatory neurotransmitters like N-methyl-D-aspartate and Ca^{2+} and Na^{+} ion channels.⁷⁰ Excessive intracellular Ca^{2+} may further triggers cascades that attack the lipid bilayer by activating calcium-dependent phosphorylases.⁷¹ Laboratory and clinical studies have shown proportional increases in glutamate with injury severity and persistent elevation of glutamate in the weeks following injury has also been associated with high mortality rates.^{72,73}

Mitochondrial damage is initiated by ischemia, the influx of Ca^{2+} in the cytosol and the increased presence of reactive oxygen species. Disruption of the mitochondria is a major focal point of TBI research as it inhibits the production of ATP, further contributing to the energy crisis, and leads to various forms of cell death. Apoptosis and

necrosis are the primary mechanisms of cell death and both are heavily influenced by mitochondrial dysfunction.⁶⁶ Apoptotic cell death is initiated by the opening of the mitochondria permeability transition pore which releases apoptotic molecules such as cytochrome-c that activate caspases that trigger the final apoptotic process.⁷⁴ Similarly, necrosis is characterized by damage to organelles and cellular swelling and leads to the release of cellular contents beginning the inflammation processes.⁷⁵

Neuroinflammation is a complex process of events initiated at the point of injury when tissue damage leads to danger associated molecular patterns. These molecular patterns are bound by pattern recognition receptors that are recognized by ligands and trigger the production of pro-inflammatory cytokines. Inflammation plays a dual role in TBI as it has been shown to mitigate detrimental and repair processes in the central nervous system (CNS) and is further complicated by the role of competing anti-inflammatory processes.⁶⁶ The similar process of brain swelling, or edema, is caused by disruption to the blood brain barrier (BBB) and the accumulation of fluid. Edema is a regularly reported symptom of TBI and typically results in increased intracranial pressure and in severe cases it can significantly restrict the supply of blood and oxygen to the brain.⁷⁶

1.5 Laboratory Injury Models

Animal models have played a critical role in the understanding of TBI with rodent models being the most studied by far. To understand the heterogeneity of TBI a vast array of rodent injury models have been used to mimic different severities and types of head injuries. In the laboratory setting rodent injuries are commonly induced using either CCI,

weight drop, or LFP methods. Each of these methods can be used to generate mild, moderate, or severe injuries reproducibly. Each model produces minor differences in brain pathophysiology and only through the building of a common framework from many different injury models can the scientific community begin to understand TBI.²²

CCI methods use a pneumatically or electromagnetically driven piston at a controlled velocity to induce a focal injury with a specific amount of head displacement. First usage of the CCI model was performed in 1988 by Dr. James Lighthall for use on ferrets, but by 1991 CCI models were extended to the most common modern usage of inducing injuries in rats.^{77,78} The piston of the CCI device is attached to a rod that is typically driven into open brain tissue following a craniotomy, but CCI methods are also used extensively to study closed head injuries.^{79,80} Impact of the rod onto open brain tissue or the closed skull of the animal induces injury through the rapid compression of brain tissue causing damage to the cortex or even subcortical structures in higher severity injuries. The tip of the rod varies in size and geometry for scalability to different rodent species and within some limits the CCI device can be controlled for velocity, depth, and duration of injury.²⁶ After injury, a contusion core develops over time around the region of damaged cells which is often visible a few days after injury.⁸¹ Mild TBI models induced with CCI have been shown to exhibit behavioral and learning defects, both of which are reported to be magnified and longer lasting in severe TBI models.⁸²

LFP injury models are among the best-characterized and reproducible brain injury models. Depending on the injury parameters LFP models can induce diffuse injuries or diffuse injuries with focal components.²⁷ LFP models originated in the 1940's and were applied to rodent models toward the end of the 1980's.⁸³ Injury from LFP models is

generated via the rapid injection of fluid, typically saline, through a craniotomy into the epidural space which causes the brain to move inside the skull and brain tissue deformation.⁸⁴ Mild TBI induced via LFP presents a low level of cell death and have been shown to cause some short-term behavioral impairments whereas severe injuries often show pronounced cell loss and long-lasting behavioral deficits in animal models.

Weight drop methods are the most established and commonly used method for inducing diffuse TBI in laboratory models. Weight drop reached a height in popularity in the 1990s but publications using this method have since plateaued in favor of more modern methods such as LFP and CCI.²² Weight drop methods require the use of a weight dropped from a specific and known height through a tube onto to the top of the closed skull. Varying degrees of injury are induced by changing the mass of the weight, drop height, surface beneath the animal, or by protecting the skull of the animal with a helmet.^{85,86} The greatest advantages of weight drop methods are in its ease of implementation as well as its ability to quickly produce repeat injuries.⁸⁷

Blast injuries while uncommonly induced in laboratory settings, have received growing attention largely from media coverage of military personnel with combat injuries. Laboratory methods for inducing blast injuries utilize shock tubes which are filled with a compressed gas to mimic the negative pressure of blast waves.^{88,89} Blast injuries are most easily categorized as diffuse injuries and consist of numerous small deformations across different regions of the brain. The four basic mechanisms for classifying blast injuries are primary, secondary, tertiary, and quaternary. Primary blast injuries are the result of over-pressurization from high energy explosives and commonly result in pulmonary barotrauma, middle ear rupture, and abdominal hemorrhaging.

Secondary and tertiary injuries are caused by flying debris or fragments and individuals being thrown by blasts, respectively. Finally, quaternary injuries include all injuries resulting from blasts not captured in the previous three levels and most commonly include exacerbation of previous conditions.⁹⁰ All four levels of blast injury often result in either closed or open brain injury and concussions.

CHAPTER 2

BIOMARKER STUDIES

2.1 Biomarker Research

Biomarkers serve as objective indicators of variation from normal biological function including exposure and intervention events. They may act as surrogate endpoints to clinical trials and may, in rare cases, substitute for clinically relevant endpoints.⁹¹

Biomarkers may be diagnostic tools for identifying the cause of a disease, prognostic in informing the likelihood of potential outcomes, or predictive of various disease states.^{92,93}

TBI's heterogeneous nature has made establishing a universal panel of biomarkers particularly challenging. Features which fluctuate significantly at the onset of injury may not translate well to long term outcomes and thus make them difficult to use as a predictive measure. The exploration for potential biomarkers of TBI has focused primarily on proteins but has also been extended to micro-RNA (miRNA) and to lipid metabolites which is the focus of this thesis.

Studies of protein biomarkers have increased dramatically over the past decade, but are often limited to cases where the BBB is disrupted allowing proteins to migrate from the cerebral spinal fluid (CSF) into the blood.⁹⁴ Protein biomarkers, particularly glial and neuronal proteins like GFAP and UCH-L1, have received considerable attention and show potential as TBI biomarkers over a range of injury severities. GFAP levels in human serum have been shown to correlate with GCS scores and brain imaging findings in severe and moderate-mild TBI patients.^{95,96} Similarly, elevated levels of UCH-L1 have also been shown to correlate with imaging results, injury severity, and the need for

neurosurgical intervention in mild to severe TBI patients.^{97,98} In 2018 GFAP and UCH-L1 received FDA approval as a blood-based biomarker assay for predicting intracranial hemorrhaging in patients with mild TBI.⁹⁹ The neuronal protein tau has also been studied heavily as a biomarker candidate for TBI, the natively unfolded protein is localized in neurons and has high concentrations in the CSF. This protein has been of particular interest in TBI studies because, when cleaved into c-tau, it is able to permeate the BBB and enter the CSF and blood.¹⁰⁰ The greatest challenge of studying this protein lies in its short half-life; however, recent work has shown large increases of tau in the plasma of concussed humans over those without injury.¹⁰¹ While these proteins and others have shown some success in distinguishing TBI patients from controls, routine clinical use of biomarkers for the consistent diagnosis of TBI over a range of severities has not yet been accomplished.

miRNA are short 19-28 nucleotide sequences which are noncoding RNA molecules used to regulate protein synthesis.¹⁰² miRNA's high expression in the brain, ability to permeate the BBB, and their stability in peripheral biofluids make them ideal candidates for prognosis and therapeutic TBI decisions.¹⁰³ Candidate miRNA biomarkers have been explored for alterations in the blood, CSF, and saliva of TBI patients across a range of severities and timepoints. Among the largest human studies conducted examining miRNA (n=114) researchers found increased levels of miR-93, miR-191, and miR-499 to peak in the serum of injured patients at 2- and 7-days post injury.¹⁰⁴ Similar changes in the miR-30 family have been reported in both the blood and saliva of mild TBI patients.^{105,106} Decreased expression of miR-30 has been associated with cell morphology, loss of cellular adhesion and tight junction disruption and therefore may

play a role in maintaining the BBB.¹⁰⁷ miRNA, like lipid biomarkers of TBI, are in their infancy compared to protein biomarkers but may one day guide medical decisions for treating patients.

Lipids are a large class of cellular components with vast diversity, signaling roles and structures. Recent developments in instrumentation and bioinformatics has led to the rise of lipidomics, a sub-field of metabolomics, which has allowed for insight into the dynamic and complex changes of the lipidome in disease states. Lipids are grouped into categories based on structure and include fatty acyls, glycerolipids, glycerophospholipids, sphingolipids, sterol lipids, saccharolipids, polyketides, and prenol lipids.¹⁰⁸ The CNS contains thousands of different lipids species, most of which are synthesized in the brain and separated from peripheral biofluids by the BBB.¹⁰⁹ Alterations to the lipidome following TBI have been increasingly reported in recent years and are the focus of the research presented in this thesis.^{110,111} Identifying the complete lipid signature of TBI will require experimental research of peripheral biofluids such as serum, urine, saliva, and CSF and the study of central components such as brain tissue over a range of severities and post injury timepoints.

The CNS is highly enriched in fatty acids which are the building blocks for complex lipid species and increase in abundance as phospholipids degrade. Fatty acids have a variety of chain lengths and can be saturated, monounsaturated, or polyunsaturated.¹¹² Arachidonic acid and docosahexaenoic acid are polyunsaturated fatty acids with significant structural and signaling roles that create lipid mediators such as the eicosanoids and docosanoids.^{113,114} A study of the CSF following TBI in human patients (n=15) showed significant increases in the concentrations of all free fatty acids with

p<0.001 for arachidonic and docosahexaenoic acids 48 h after injury.¹¹⁵ Additional work from the same group showed similar increases in fatty acid concentrations from patients with subarachnoid hemorrhage, indicating that increased free fatty acid concentrations were not necessarily unique to TBI.¹¹⁶ Previous experimental work in the group conducted on Sprague-Dawley rodents also revealed a statistically significant increase of arachidonic acid at 3- and 7- days post injury between injured and control groups.¹¹¹

Phospholipids (PL) comprise approximately 45% of the dry weight of the brain and contain a glycerol backbone with hydroxyl groups in the sn-1 and sn-2 positions linked to fatty acids. PL species including phosphatidylethanolamines (PE), phosphatidylcholines (PC), phosphatidylserines (PS), and phosphatidylinositols (PI) vary based on polar head groups located at the sn-3 position.¹¹² Of the phospholipids, PE and PC have the highest presence in white matter (19.6% and 11.8% respectively) and in grey matter (30.7% and 25.1% respectively).¹¹⁷ Studies of human CSF from patients with GCS scores below 8 have revealed significant increases in PE, PS and PC when compared to patients with suspected neurological disorders.¹¹⁸ Similar experiments in patients with GCS scores ranging from 3-11 showed an increase in all PL species at nearly all measured timepoints in injured patients over controls. Interestingly PL abundance was greatly increased in patients who died from their injuries when compared to those who survived.¹¹⁹ A detailed study of plasma from soldiers who sustained mild TBI several years prior to analysis showed significant decreases in PC, PE, and PI when compared to soldier without head injuries.¹²⁰

The hydrolysis of PL by phospholipases cleaves acyl residues and produces lysoPL species which aid in the regulation of numerous biological processes.¹²¹ LysoPC

species for example play a role in pro-inflammatory processes in the nervous tissue. Glycerolipids contain a glycerol backbone with varying numbers of fatty acyl residues and species like the diacylglycerol 2-arachidonoylglycerol can act as a source of neuroactive endocannabinoids which affect neurogenesis and synaptic plasticity.^{122,112} Sterols like cholesterol are an important component of cell membranes and in a human study of CSF (n=27) non-esterified cholesterol exhibited a 5-fold increase in severe TBI patients over controls.¹¹⁰ Cardiolipins are another species of lipid which is highly enriched in the brain, but has seen little research in the serum of TBI patients. In rat plasma cardiolipins only constitute approximately 0.001% of all PL species, however LC-MS analysis of brain tissue homogenate from a human patient with severe TBI showed a large presence of oxidized cardiolipins from the right temporal lobe.¹²³

The study of potential biomarkers of TBI has revealed a complex array of changes in the blood, CSF, and brain tissue of patients and experimental models. Given the heterogeneity of TBI it is unlikely that any single biomarker or type of biomarker will be able to capture all injury mechanisms alone. Series of biomarkers or biomarker panels are likely required to understand differences in injury states across a range of severities and post-injury time-points.

2.2 Metabolomics Experimental Design

Metabolomics is an umbrella term capturing all studies examining small biological molecules in an organism's metabolism with the goal of obtaining a comprehensive understanding of small molecules within an organism. The versatility of metabolomics experiments is highlighted by their ability to detect statistically significant

fluctuations between healthy and diseased states. Modern metabolomics has been heavily influenced by the field of proteomics including in the instrumentation, separation methodologies, and data processing methods used. However, important distinctions between the two exist. While the metabolome may seem less complex than the proteome, metabolites can exhibit diverse chemical structures, concentrations, polarity, and volatility.¹²⁴ The metabolome is also greatly affected by temporal fluctuations, and the presence of exogenous species such as drugs, nutrients, and toxins.¹²⁵ Many small molecules are common across species making them difficult to use for species determination but advantageous for animal model studies in that metabolite fluctuations following disease state are often similar between species.¹²⁶

Lipidomics is a subset of metabolomics that examines lipid molecule fluctuations and can be done in targeted and untargeted fashions. Untargeted approaches are designed to discover as many species as possible and to examine both unknown and known metabolites. This type of approach is useful in hypothesis generating experiments and yields a global understanding of an organisms lipidome.¹²⁷ Untargeted lipidomics experiments typically operate under the assumption that the analysis of metabolites will produce a list of identified or identifiable lipids that can be mapped to known pathways.¹²⁴ However, these methods are often challenged by difficulties in compound annotation. Despite lipid molecules containing common elements such as C, H, O, N, S and P, there is no overall common repeating alphabet, like that which exists in proteins. Validating discovered metabolites using further and often in-depth experiments is almost always necessary but will likely become less necessary as databases improve over time.

Targeted metabolomics approaches are hypothesis driven and commonly follow larger scale untargeted studies examining tens or hundreds of known metabolites that typically have some clinical interest. While these studies are often much less labor and time intensive than untargeted approaches, the potential for overlooking metabolic responses of interest is high.¹²⁴ In targeted studies, specific compounds of interest are quantifiable to laboratory standards and can be compared to well established reference ranges. The precision of targeted studies is usually greater than untargeted approaches even after correcting for issues such as time dependent signal drift.¹²⁸ The work presented in this thesis utilizes an untargeted lipidomics approach for identifying features of interest present in TBI models with the future goal of assessing potential biomarkers in targeted studies.

2.3 Mass Spectrometry

Methods using mass spectrometry (MS) have enabled quantitative and qualitative analysis of lipids in complex matrices in both targeted and untargeted manners.¹²⁹ The efforts of organizations such as the LIPID MAPS consortium have yielded regularly updated databases of high-quality lipid standards which are freely available to scientific community. MS studies are the most commonly used method for metabolomics and lipidomics experiments as they are overall the most selective, sensitive, cost effective and yield the greatest depth of coverage.¹³⁰ MS instrumentation consists of an ion source, a mass analyzer, and a detector and are often coupled to a front end separation method such as chromatography. The researcher's choice of polarity and ion source, electrospray

ionization (ESI), chemical ionization (CI), matrix assisted laser desorption ionization (MALDI), electron impact (EI) etc. allow for a wide breadth of metabolites to be analyzed. After metabolites are converted to the gas phase and ionized, they travel through a mass analyzer such as an Orbitrap, Fourier transform ion cyclotron resonance (FT-ICR), time-of-flight (TOF), quadrupole, or ion-trap that separates ions based on their mass to charge values (m/z).¹³¹ Ions then reach a detector, typically a Faraday cup, photomultiplier tube, or simply an image current where the relative abundance is recorded and sent to a digitizer that converts electrical signal to a mass spectrum readable on a computer.

Analyte separation prior to MS is typically accomplished using chromatography in either the liquid (LC) or gas phase (GC) which separates analytes based on affinity for a stationary phase. GC uses an inert carrier gas as a mobile phase to move analyte through a capillary column where a stationary phase commonly consisting of a high boiling point polymer coats the wall of the tube. Analytes are then separated based on their affinity for the column where analytes with greater attraction to the stationary phase have longer retention times and come off the column slower than analytes with a lower affinity.¹³² LC also makes use of a stationary and mobile phase and is commonly done in either normal (NP) or reverse phase (RP). NP chromatography uses a polar stationary phase and non-polar non-aqueous mobile phase and yields longer retention times for polar analytes. A commonly used variant of normal phase chromatography called hydrophilic interaction chromatography (HILIC) is useful for very hydrophilic samples such as carbohydrates which are insufficiently soluble in the non-aqueous mobile phase NP chromatography. HILIC experiments separate polar compounds based on liquid-

liquid partitioning as opposed to solely relying on adsorption to a column.¹³³ RP chromatography experiments uses a hydrophobic stationary phase commonly consisting of long chain carbon molecules fixed to beads which are tightly packed into the column and a polar mobile phase. RPLC separates lipid molecules based on lipophilicity where increasing lengths fatty acyl chains largely determine the length of time an analyte is retained on a column.¹³⁴

In a typical lipidomics MS workflow, MS1 experiments are done to generate accurate mass data for many compounds or features. These data are then used in following statistical calculations to help guide feature selection toward a small subset of potentially interesting features so additional MS2 experiments can be performed for compound identification. Advanced workflows can collect full MS1 data and MS/MS in a single experimental run. The most frequently used method for this type of data collection is done using data-dependent acquisition (DDA), where the highest abundant lipids at a time point or lipids above an abundance threshold are selected and collected for MS/MS.¹³⁵ Despite its power, a drawback of this precursor ion selection method is that it suffers from low analytical reproducibility and can select features of little biological relevance.¹³⁶ Reliance on pooled quality control (QC) or reference samples is common in this method, separating metabolite quantification from identity confirmation. Data independent acquisition methods (DIA) such as sequential window acquisition of all theoretical fragment-ion spectra involve the selection of wide, consecutive m/z windows and effectively covers the entire mass range. All ions within these windows are fragmented together at one time, but due to the width of isolation windows which are typically between 10 and 50 Da, linking precursor ions to corresponding fragments is

difficult. This method of MS2 collection can make interpretation of unknown metabolites significantly more challenging than DDA methods.¹³⁵

2.4 Imaging

Imaging mass spectrometry (MSI) has seen significant growth as an investigative tool for metabolomics experiments and yields spatial distribution information unobtainable through LC-MS and NMR methods. Matrix assisted laser desorption ionization (MALDI), secondary ion mass spectrometry (SIMS), and desorption electrospray ionization (DESI) are the most widely used MSI tools for metabolomics. MALDI MSI was first described in 1994 by Bernhard Spengler and further developed by Richard Caprioli in 1997.^{137,138} In this technique the biological sample is covered in an organic matrix, typically containing an organic core, which is designed to absorb energy from an UV laser beam ion source. The energy absorbed by the matrix causes an explosive desorption of analyte together with matrix crystals and after a short time delay a voltage differential is applied bringing ions into the mass separating portion of the instrument. MALDI paired with TOF mass analyzers to separate ions are the optimal MALDI IMS platform allowing for a high mass range around 100,000 Da and lateral resolution as low as 10 μm .¹³⁹ This soft ionization technique makes the spectral information collected less complicated than harder ionization sources and allows for a larger mass range than other methods.

SIMS was developed in the beginning of the 1960's and uses a beam of primary ions which transfers collisional energy to molecules on the surface of the analyte. This technique uses a harder ionization source than MALDI as the energy of primary ions is

considerably higher than the covalent bonds on the surface of the analyte leading to considerable fragmentation. The mass range of SIMS is limited to approximately 1,000 Da and only about 1% of all molecules retain an electrical charge and can be detected by an analyzer.¹³⁹ The spatial resolution of SIMS can reach below 10 μm and modifications to extend the mass range including matrix application and thin metal layer coatings have been studied to extend the uses of this technique. DESI is a newer soft ionization MSI method first reported in 2004 and highly advantageous in that it allows for ambient and direct analysis of tissue, liquids, frozen solutions, or adsorbed gases.^{140,141} In this method charged microdroplets are generated from a solvent inside the emitter of the electrospray ion source. These microdroplets then form a thin film on the surface of the analyte and dissolve the top layer. Secondary droplets containing analyte are produced after new primary droplets impact the dissolved analyte and transport the analyte to the surface the MS inlet. This method has high sensitivity, nearly instantaneous response time, and a larger mass range than SIMS but spatial resolution is poor and rarely better than 100 μm .¹³⁹

2.5 Nuclear Magnetic Resonance

Behind mass spectrometry, NMR is the most widely used technique in metabolomics studies. Briefly, this method works by placing molecules in a strong magnetic field and measures the resonant frequencies of nuclei which can then be converted to an NMR spectrum. Compared to mass spectrometry, NMR requires much less elaborate sample preparation measures and does not require separation of metabolites prior to analysis. NMR allows for rigorous quantitation of highly abundant metabolites

and offers an advantage for metabolites which are difficult to ionize.¹⁴² NMR is also non-destructive to samples and offers enhanced reproducibility of experiments making it an attractive option for many researchers. Stable isotope labeling allows NMR to annotate the dynamics of metabolite transformations and can be used to explore the compartmentalization of metabolic pathways.¹⁴³

NMR is limited to the study of a small number of metabolites, approximately 100-200, per single experiment and typically yields limits of detection which are 10 to 100 times worse than mass spectrometric methods. Additionally, NMR often requires specially trained operators to work on large, expensive instruments that are difficult to maintain and often located in centralized core facilities. The selection of instrumentation is often dictated by cost, accessibility, and availability of experts to process samples. Ultimately the choice of platform for metabolomics studies should rely on the nature of samples and focus of the study.¹⁴⁴ Currently there is no method capable of identifying and quantifying all metabolites in a sample, thus a combination of approaches are needed to gain the best overall understanding of complex biological systems.

2.6 Data Workflow

Metabolomics experiments require many steps to go from hypothesis to biological interpretation. A typical experimental workflow requires planning, sampling, sample pretreatment, instrumental analysis, data processing, multivariate modeling, and interpretation. Typical metabolomics experiments use hundreds or even thousands of samples which all must be collected and pretreated meticulously, and often require significant instrument run time and complex modeling before interpretation of results can

begin. The time needed to conduct sampling, sample treatment and instrumental analysis can span weeks, months, and even years depending on sample size.¹⁴⁵ Each step in the process is important as the result is only as strong as the weakest link in workflow. Standardized protocols exist for most sampling, pretreatment, and instrumental analysis steps however data processing and multivariate analysis methods are often selected by user preference or default program settings.¹⁴⁶

Normalization methods should be used during pre-processing to help limit error and are commonly classified into three groups: (i) data driven methods, (ii) internal standard (IS) based methods, and (iii) quality control (QC) based sample methods.¹⁴⁷ The first group of normalization methods relies on self-averaging properties or that increases in a metabolite in one sample will be matched by decreases of the same metabolite in other samples. This assumption is not necessarily valid in all lipidomics experiments as changes in solvent pH or temperature may affect some lipid species differently than others. IS methods require either internal or external standards be added to samples to normalize each metabolite. IS method accuracies are hindered when compounds co-elute with IS, when peak heights of IS do not describe all matrix effects, when IS are sensitive to their own obscuring variations, and when the structural properties of IS do not include all species in a lipidomics dataset. QC methods usually require small aliquots of each sample to be combined into a single pooled sample to create a matrix like that of each sample. In recent years QC methods have grown in popularity partially due to low cost, ease of implementation, and their ability to decrease unwanted error while still maintain biological variation. QC samples are placed throughout the experiment commonly at the beginning and end of batches to control for instrument drift over time.¹⁴⁸ While

promising, QC methods rely on the assumption that all systematic error is related to batch effects, run order, or processing sequence and do not consider correlation of error between compounds.

Practical considerations yield a need for variable scaling prior to data analysis. The linear combination of experimental observations from different instruments such as NMR and MS have no physical meaning as units differ, however even when variables have the same units, disparate intensities and variances between variables cause multivariate feature selection methods to focus on a small subset of highly intense features.¹⁴⁹ Data scaling provides a solution to this problem as methods such as auto-scaling force features to have a mean of zero and unit variance and allow multivariate models to examine correlations rather than covariances. Numerous forms of scaling exist and commonly include pareto scaling whose goal is to reduce the importance of large values and range scaling whose goal is to compare metabolites relative to a biological response range.¹⁵⁰ The greatest disadvantage of scaling lies its tendency to amplify instrumental noise, but this can be mitigated through baseline removal, removal of features with large variation, and removal of features present in of a small percentage of samples.

The flexibility of multivariate analysis allows for a variety of instrumental approaches. Almost universally, data is input into a data matrix X containing N observation row vectors of K variables in each vector with almost no constraints placed on the values within.¹⁴⁹ Following pre-processing steps matrix X can be decomposed directly through unsupervised methods such as principal component analysis (PCA) or it can be paired with a class matrix Y for supervised dimensionality reduction in the case of

partial least squares regression (PLSR) and its descendants. Binary class membership information in the Y matrix allows for forms of discriminate analysis (DA) such as PLS-DA and orthogonalized PLS-DA.¹⁵¹ The primary goals of PCA and PLS are to identify class differences in a multivariate dataset, where classes refer to biological considerations such as injured and uninjured rat serum as in the case of this thesis.

Feature selection is common in metabolomics experiments as there are significantly more variables, for example m/z, RT pairs than there are N. Thus, variable selection may be beneficial in selecting biologically meaningful regions of a dataset. Exhaustive variable selection methods may apply recursive algorithms, support vector machines, genetic algorithms, or random forests to select variables pertinent to class separation.^{152,153} The greatest critique of these methods lies in the potential for overfitting where random variables irrelevant of a biological condition separate samples into predefined classes. Methods for reducing overfitting commonly include many iterations of permutation tests or when available the use of additional test data.¹⁵⁴ The application of prior dataset knowledge is beneficial prior to feature selection and may help further reduce the overfitting of final feature selection.

CHAPTER 3

METHODOLOGY

3.1 Chemicals

Chemicals used to prepare mobile phases and solutions included LC-MS grade water and acetonitrile (ACN) (Fisher Scientific International, Inc. Pittsburg, PA), isopropyl alcohol (IPA) (Honeywell International, Inc. Charlotte, NC), formic acid (purity > 99.5%) (CovaChem, LLC. Loves Park, IL), and ammonium formate (purity > 99.995%) (Sigma-Aldrich, Inc. St. Louis, MO). Uninjured Sprague-Dawley rat serum (ab7488) (Abcam, PLC. Cambridge, UK) was used as reference serum during LC-MS data collection and to supplement MS/MS data collection. SPLASH II Lipidomix (Sigma-Aldrich, Inc. St. Louis, MO) served as an analytical lipidomic standard for MS experiments.

3.2 Injury Protocol and Blood Collection

All procedures involving Sprague-Dawley rat models were performed in accordance with guidelines set forth in the Guide for the Care and Use of Laboratory Animals (U.S. Department of Health and Human Services, Pub no. 85-23, 1985) and were approved by the Georgia Institute of Technology Institutional Animal Care and Use Committee (protocol #A100188). Female (n=18) and male (n=14) Sprague Dawley rats (8 weeks old; Charles River) weighing between 300-400 g were kept on 12 h reverse light-dark cycles, where food and water were available ad libitum. Animal models were randomly assigned to sham-operated (n=11), single CCI (n=10), and three times repeated

CCI (n=11) groups (Figure 1A). Sham-operated animals received no injuries and were used to control for lipid fluctuations from anesthesia usage and time dependent daily cycles.

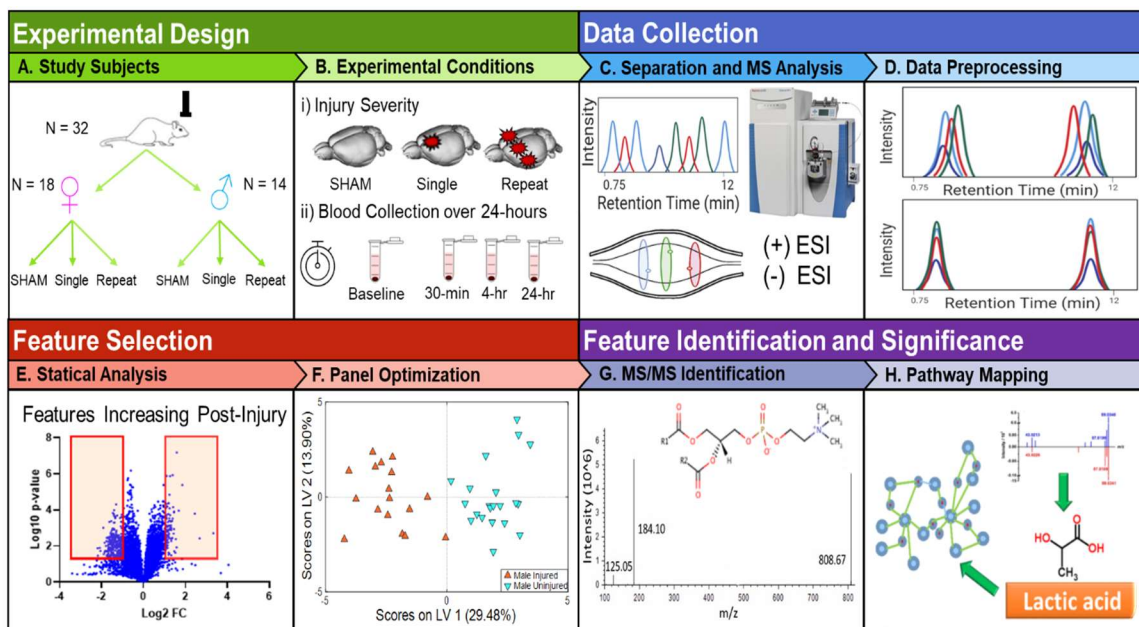


Figure 1: Overview of study design, data processing, feature selection and identification. (A) Experimental groups included both the male (n=14) and female (n=18) sexes which were randomly assigned to either sham controls, which received no injuries (n=11), single impact, which received one closed skull CCI injury (n=10), or repeat impact, which received three separate closed skull CCI injuries (n=11). (B) Whole blood was collected at baseline prior to injury and again at 30 min, 4- and 24-h post-injury. (C) Workflow illustrating data collection with LC-MS in both positive and negative ion modes yielding 14,119 features. (D) Peak alignment, picking and integration were accomplished using Compound Discoverer v. 3.0.0, (Thermo Scientific). (E) Following initial feature reduction, 499 statistically significant features of interest with fold changes above 1.5 were identified for further PCA and oPLS-DA modeling. (F) Genetic algorithms were used to create optimized reduced feature panels capable of classifying injured and uninjured serum samples at all collection timepoints. (G) Targeted MS/MS experiments were then performed to identify features present in the final optimized panels. (H) Following identification, biological significance and pathway mapping was undertaken to qualitatively understand features of interest as they relate to mild TBI.

A CCI device (Pittsburgh Precision Instruments, Pittsburgh, PA) was used to induce single and repetitive closed-head injuries to the cortex. Prior to injuries, all rat groups were anesthetized with isoflurane (induction: 5% isoflurane; maintenance: 2-3% isoflurane) and a toe-pinch was administered to evaluate loss of consciousness to ensure minimal pain during the injury process. A pneumatic piston on the CCI device with a 5 mm tip diameter was positioned 15 degrees below vertical in the coronal plane to induce injury to the closed skull 30 s after removal of the isoflurane supply. All experimental injury groups received injuries from the pneumatic piston at a velocity of 5 m/s. The single impact injury group received a one injury with 5 mm head displacement. The repeat injury group received a total of 3 injuries over 2 min intervals with head displacements of 5 mm, 2 mm, and 2 mm, respectively. Sham-operated animals received treatment identical to injured animals excluding injury procedures (Figure 1B). Following final injury, time-to-right was recorded, and animals were monitored to survey the presence of neurological deficits.

Whole blood was collected from all study subjects at baseline prior to injury (n=29), 30 min post-injury (n=25), 4 h post-injury (n=32), and 24 h post-injury (n=28). Approximately 200 μ L of whole blood was collected from the tail artery with 22-gauge Precision Glide needles (Beckton Dickson) and stored on ice. Whole blood was left at room temperature to coagulate for 45 min and sample collection followed guidelines for limiting potential hemolysis. Samples were then centrifuged at 4 °C for 15 min at 2500 g, and serum was collected and stored at -80 °C (Figure 1B).

3.3 Serum UHPLC Analysis

Serum samples were thawed on ice for one hour prior to the addition of IPA and Splash II Lipidomix in (1:3 v/v) to separate lipids and small non-polar metabolites. Serum and IPA mixtures were vortexed for 10 s, centrifuged at 16000g for 7 min and the supernatant was collected for LC-MS analysis. Sample blanks were prepared with 50 μ L of LC-MS grade water, and pooled QC samples were formed from 5 μ L aliquots of all study subject serum samples. Reference samples were collected from commercially purchased uninjured Sprague-Dawley rat serum and were processed in the same manner as study subject serum samples. All samples were run in a randomized order over two and a half days of consecutive instrument time. QC samples were placed every 24 runs to evaluate system stability and to account for time dependent batch effects.

RP chromatography was preformed using a Vanquish Horizon UHPLC (Thermo Fisher Scientific, Inc., Waltham, MA) instrument run in both positive and negative ion modes. Both ion modes used identical two-part mobile phases. Mobile phase A was a (40:60 v/v) water/ACN mixture and mobile phase B was a (90:10 v/v) IPA/ACN mixture. Both mobile phases contained 0.1% formic acid and 10 mM ammonium formate solution as a buffer. The stationary phase used for both ionization modes was a 2.1 x 50 mm Accucore C30 column with 2.1 μ m particle size. An ID-X Orbitrap Tribrid mass spectrometer (Thermo Fisher Scientific, Inc., Waltham, MA) was used following separation for all samples over a scan range of 150-2000 m/z (Figure 1C).

3.4 Data Processing

Raw spectral data from LC-MS experiments were pre-processed using Compound Discoverer v3.0.0 software (Thermo Fisher Scientific, Inc., Waltham, MA). Initial steps involved retention time peak alignment between samples, peak area integration, peak picking, and QC area normalization (Figure 1D). Features eluting with the solvent front or having retention times below 0.75 min were removed to account for potential ion suppression effects.¹⁵⁵ Further reduction removed features not present in at least 75% of samples at concentrations above five times the baseline abundance and features with coefficients of variation (CV_m) greater than 20% in QC samples. A combined set of 14,119 spectral features 3,646 and 10,473 from the negative and positive modes respectively were obtained.

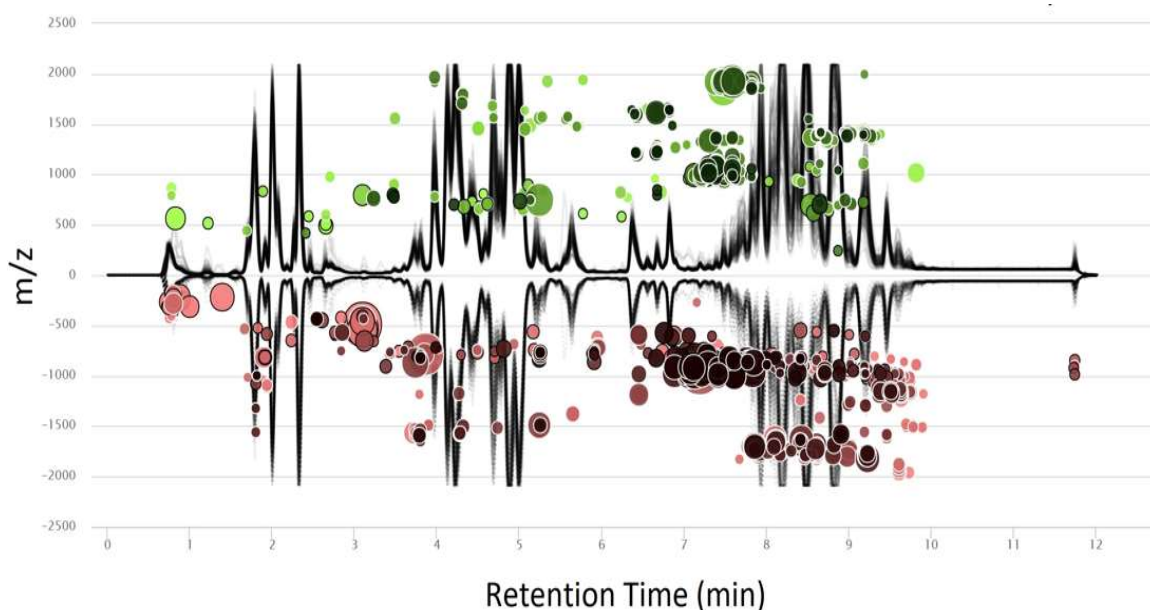


Figure 2: Cloud plot generated in the XCMS web-based application showing positive ion mode retention time versus m/z for features with high fold change and statistical significance between injured (green) and uninjured (red) animals. The black traces outline chromatographic retention time on the x-axis and m/z values on the y-axis for each sample. Each bubble in the plot corresponds to one metabolite feature with fold change at or above 1.5 and a p-value at or below 0.05 using a Welsch's t-test. The color and size of each bubble denote the directionality and magnitude of fold change respectively with larger bubbles representing larger fold changes. The darkness of color in each bubble represents p-value significance with darker colors corresponding to features with greater statistical significance. Features with large m/z values are truncated for ease of visibility.

The XCMS Online cloud-based informatic platform was used to visualize differently expressed features in injured versus uninjured serum samples in the positive (Figure 2) and negative (Appendix A) ion modes. Features of interest were identified as those exhibiting fold changes greater than 1.5 and having Benjamini Hochberg adjusted p-values < 0.05 after Welsch's t-testing (Figure 1E).^{156,157} Further reduction to the feature of interest panel was done by evaluating median ratios of normalized area between all injury timepoints and baseline values. Features with ratios differing by less than 20% between injured and sham operated animals at all post-baseline timepoints were removed

to better account for lipidome changes not induced by TBI. Preliminary feature reduction led to a panel of 499 features, 76 in the negative ion mode and 425 in the positive ion mode which were exported as a single matrix into MATLAB (MATLAB R2019a, The Mathworks, Natick, MA, with PLS Toolbox v8.1.1, Eigenvector Research, Inc., Wenatchee WA).

Optimized feature panels for classifying injured and uninjured serum groups were created using genetic algorithms (GAs) on male and female sera separately. Genetic algorithms are a popular evolution-inspired approach to optimization where features are selected according to their fitness.^{158,159} The total number of times a feature is chosen is proportional to its relative fitness so features with the highest frequency are selected for the final optimized models. Detailed parameters for genetic algorithm feature selection are provided in the supporting information (Appendix A). The optimized feature panels were evaluated for discriminating power through supervised orthogonal partial least squares discriminant analysis (oPLS-DA) and tested for overfitting using 200 iterations of permutation tests (Appendix A).¹⁶⁰ Data was preprocessed by autoscaling prior to PCA and oPLS-DA analysis and cross-validated with 10 iterations of Venetian blinds cross-validation.

3.5 Discriminant Feature Identification

Identification of all features in the optimized feature panels was attempted with tandem MS analysis using normalized collision energy values of 10, 30, and 50 eV. Ion adducts and elemental formulas were generated within Compound Discoverer v3.0.0 with elements constrained to C, H, O, N, S, and P. Tentative feature identities were generated

by comparing MS/MS fragmentation patterns to entries in an in-house database, Lipid Maps, Metlin, and Human Metabolome Database (HMDB) databases using both accurate mass and generated elemental formulas with mass tolerances of 10 mDa.^{161,162,163,164} The MS/MS prediction tool within Lipid Maps was also used to further support feature identification. Fragmentation patterns were manually analyzed in some cases to differentiate various species. Low abundance species were targeted for MS/MS analysis using an inclusion list containing possible adducts of target ions.

CHAPTER 4

RESULTS AND DISCUSSION

4.1 Initial Exploratory Analysis

Serum from 32 Sprague-Dawley rats was analyzed to examine lipidome changes resulting from closed-head mild CCI prior to injury and again at 30 min, 4 h, and 24 h post-injury. Sera from female rat ID. No 15 were discarded due to errors during sample preparation and three additional sera samples were removed as outliers in T^2 and Q residual PCA plots reducing the number of sera samples analyzed to 108. The 14,119 features produced from combining the positive and negative ion mode data after initial data processing were used for unsupervised PCA (Figure A1). Pooled QC samples grouped together in the center of all study subjects, indicating an accurate representation of the average composition of study subject serum. Additionally, clear separation and tight grouping of uninjured reference serum further validated data collection. When QC and reference serum were removed, separation of samples along the diagonal of the first and second PC's revealed that a large portion of the total variance in the data was explained by lipidome differences between sexes.

A reduced 499 feature list, produced from significant features with high fold change, was also used to evaluate all study subject sera in an unsupervised manner (Figure 3). Again, minimal overlap between female and male serum samples in the reduced feature list revealed a need for separate analysis of samples by sex. Overlap between injured and uninjured serum samples occurred primarily from early post-injury blood collection timepoints, but injured samples generally corresponded to lower scores on PC1 and uninjured serum generally corresponded to higher scores on PC1. Overlap

between injured and uninjured samples showed that accurate discrimination of subtle differences in TBI pathophysiology would require supervised classification methods.

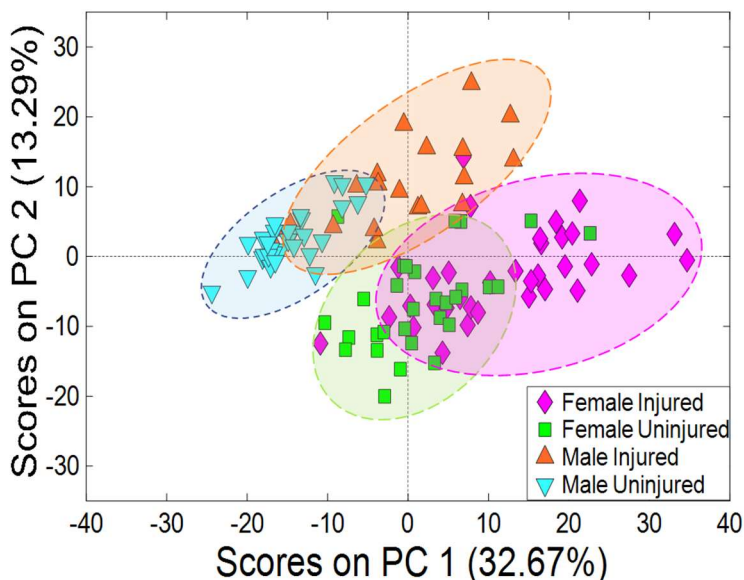


Figure 3: Unsupervised PCA scores plots of the 499-feature list of statistically significant features obtained following filtering and list reduction but prior to final feature panel selection. The distribution of samples shows separation between male and female sexes along the diagonal of PC1 and PC2 explaining a combined total of 45.96% of the variance. Male injured serum is depicted with orange triangles and male uninjured serum is depicted as blue triangles. Female injured serum is shown as pink diamonds and uninjured female serum is shown as green squares.

Previous work in the group identified a five-feature panel capable of differentiating male Sprague-Dawley rat sera of single closed head CCI at 24 h post injury and control sera with 89.3%, 91.6%, and 86.8% accuracy, sensitivity, and specificity, respectively. From the metabolomics methodology perspective, the main differences between the previous unpublished study and the study discussed here include the addition of female serum samples, repeat CCI injury serum samples, and blood collection at the 30 min and 4 h post-injury timepoints. The single injury models used in the previous study were carried out in a similar fashion to those in the current study however, they were only evaluated at

the 24 h timepoint and were not used to assess repeat CCI injuries. The panel consisted of PC species, PC(16:0_22:5) and PC(18:1_20:4), PC(18:0_22:4) and PC(41:2), which increased following injury as well as arachidonic acid and cholesterol sulfate which both decreased. To understand the ability of the previous panel to classify the animals used in this study, male serum samples from all injury severities and blood collection timepoints were evaluated using the features discovered in the previous panel and used to generate an oPLS-DA model (Figure 4).

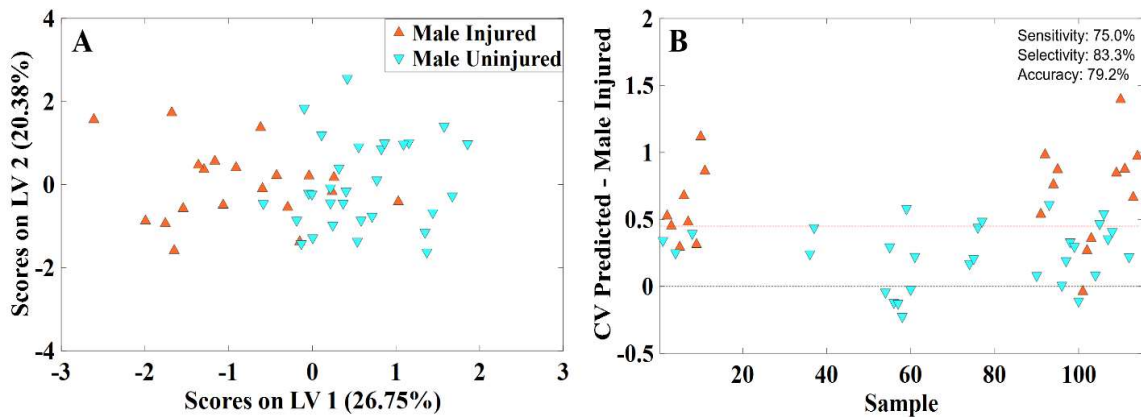


Figure 4: (A) oPLS-DA scores plot showing classification by the 5-feature optimized panel derived from previous work differentiating male single impact CCI from uninjured serum samples. (B) oPLS-DA cross validated classification plot using the same 5-feature panel. Male injured and uninjured sera are shown in orange and blue respectively with all injury classes and timepoints present in the model. The model performed with 75.0%, 83.3%, and 79.2% cross validated sensitivity, selectivity, and accuracy.

Negative scores on the first latent variable generally corresponded with injured samples while positive scores generally corresponding to uninjured samples. The model performed with reasonable sensitivity, selectivity, and accuracy warranting further investigation of these features as potential biomarkers for repeat CCI injury models. Three of the misclassified injured samples corresponded to blood collected at the 30 min

timepoint and the remaining misclassified injured samples were from a single injury rat ID No. 6 which exhibited a high degree of hemolysis during sample preparation.

Table 1: Annotation of lipids in the 5-feature panel. Retention time, observed exact mass with instrumental error, observed adduct, predicted elemental formula, and average fold change (FC) of TBI versus sham sera are reported. Positive FC corresponds to increased abundance in injured serum versus uninjured samples. All features were confidently matched to known compounds from local databases.

Feature Number	Feature ID	Retention Time (min)	m/z mass error (ppm)	Adduct	Elemental formula	FC (TBI vs. sham)
12	Cholesterol Sulfate	2.750	465.30470 1.850	[M-H] ⁻	C ₂₇ H ₄₆ O ₄ S	1.29
53	PC(16:0_22:5) PC(18:1_20:4)	4.237	852.57605 0.729	[M+HCO ₂] ⁻	C ₄₆ H ₈₂ NO ₈ P	1.11
111	Arachidonic Acid	2.482	303.23309 2.300	[M-H] ⁻	C ₂₀ H ₃₂ O ₂	1.29
250	PC(18:0_22:4)	5.511	882.62329 1.035	[M+HCO ₂] ⁻	C ₄₈ H ₈₈ NO ₈ P	1.47
7019	PC(41:2)	6.771	856.67908 -0.483	[M+H] ⁺	C ₄₉ H ₉₄ NO ₈ P	1.12

4.2 Multivariate Classification Performance

GA feature selection was used on the reduced 499 significant feature list to obtain smaller and more robust feature classification panels capable of differentiating injured and uninjured serum. Male and female serum were separated into two training sets prior to feature selection. The final feature panels were used to create oPLS-DA models and evaluated for over fitness using 10 iterations of Venetian blinds cross validation and 200 iterations of permutation tests. The male training set (n=50) was reduced to a 16-feature panel and used to create an oPLS-DA model with 2 LV. This model yielded 85.5%, 93.3%, and 89.2% cross-validated sensitivity, selectivity, and accuracy with a total of 5 misclassified samples (Figure 4 A-B). The three misclassified injured samples included two samples from a single impact rat ID No. 6 at the 30 min and 24 h timepoints as well

one sample from a repeat impact rat ID. No 11 at the timepoint 4 h timepoint. Misclassified samples all exhibited a visible degree of hemolysis following sample preparation but were retained for analysis as they were not identified as outliers in T^2 and Q residual PCA plots. To support a lack of evidence for overfitting, 200 iterations of permutation tests were run and evaluated with Wilcoxon, sign, and Rand's t-tests which all showed no evidence for overfitting at the $\alpha = 0.005\%$ confidence level (Figure A3). In the same manner, the female test set ($n=58$) was reduced to a 17-feature panel and used to create another oPLS-DA model with 4 LV and 93.5%, 92.6%, and 93.1% cross-validated sensitivity, selectivity, and accuracy (Figure 4 B-C). In this model, five total samples were misclassified including two samples from a single impact rat ID No. 13 at the baseline and 30 min timepoints, the three remaining misclassified samples arose from 30 min blood collection timepoints from repeat and sham injury models and can likely be attributed to the subtle injury boundary during the initial phases of TBI. Permutation tests for this model also yielded no evidence for overfitting at the $\alpha = 0.005\%$ confidence level (Figure A3).

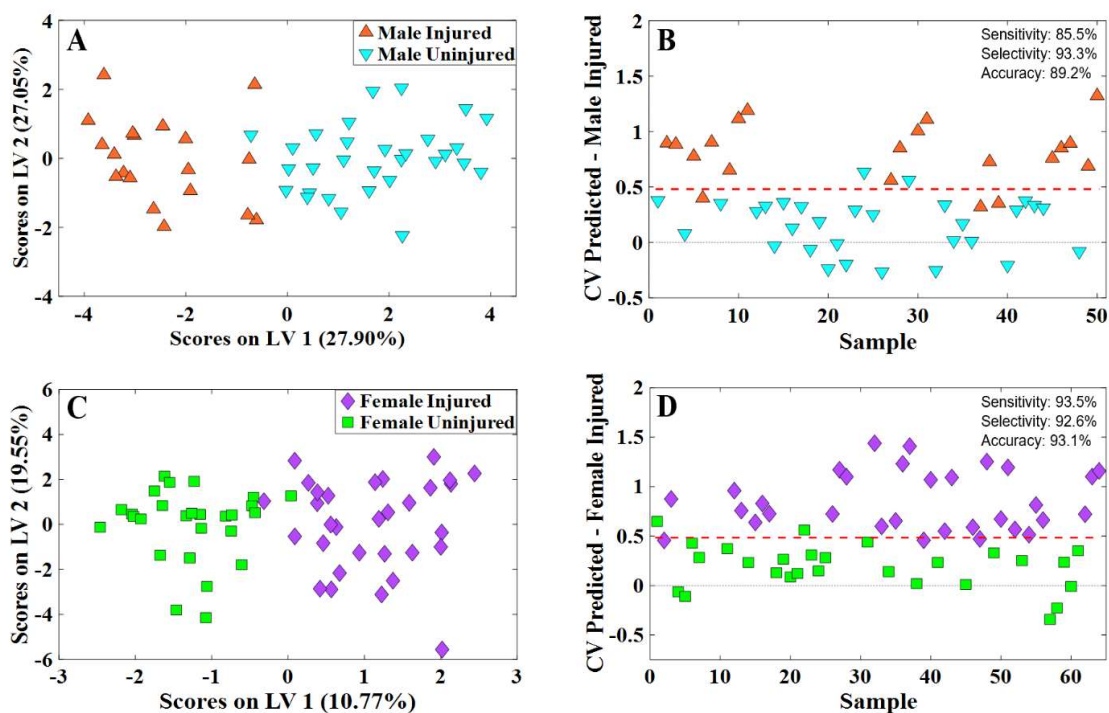


Figure 5: (A) oPLS-DA scores plot showing the 16-feature optimized panel to differentiate male injured and uninjured serum samples. (B) oPLS-DA cross validated classification plot using the same 16-feature panel. (C) oPLS-DA scores plot showing the 17-feature optimized panel to differentiate female injured and uninjured serum samples. (D) oPLS-DA cross validated classification plot using the same 17-feature panel for female sera. Both panels were evaluated with 10 iterations of Venetian blinds cross validation and 200 iterations of permutation tests which both supported a lack of evidence for overfitting (Figure A3).

The 10 common features present in the final panels of both sexes were used to create a series of oPLS-DA plots using 2 LVs to evaluate serum separation at all four blood collection timepoints. Significant overlap of samples at baseline prior to injury indicate that the markers selected in the final panels were not specific to individual animals but rather to the time progression of injury. Single impact serum samples showed the greatest degree of overlap with other injury classes and was the most misclassified class of serum at all post-injury timepoints. Overlap of single impact injury serum was relatively even between repeat and sham classes at the 30 min post injury timepoint

potentially indicating a delay in the onset of feature fluctuation for single impact serum samples when compared to repeat injury serum. The later post injury timepoints revealed greater similarity between single injury and repeat injury at the 4 h timepoint but greater overlap with sham by 24 h indicating a need to study a larger number of acute injury timepoints prior to 24 h for less severe injury models. Separation between sham and repeat injury sera grew over the time course of the study with no overlap between the classes at the final 24 h timepoint. Further investigation of these features at timepoints beyond 24 h is needed to determine the robustness of these alterations beyond 24 h post injury.

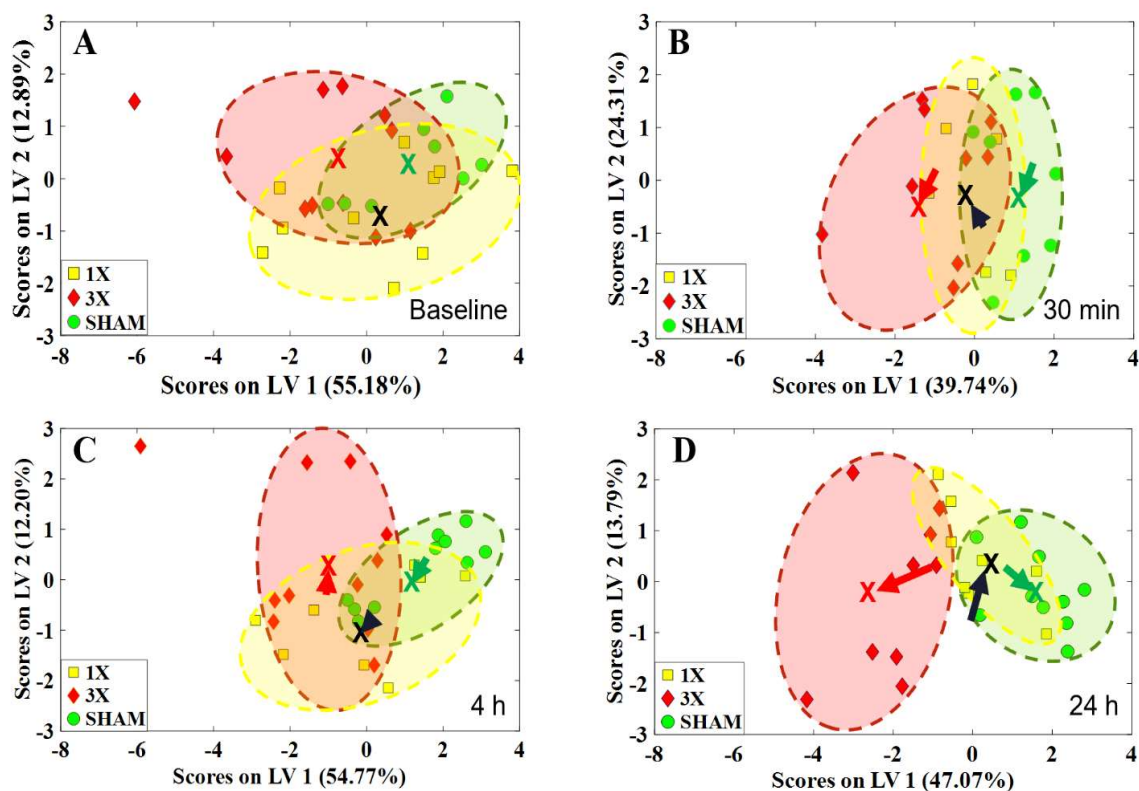


Figure 6: oPLS-DA scores plot showing the 10-features present in both final panels used to classify injured and uninjured sera at baseline (A) and 30 min (B), 4 h (C), and 24 h (D) post-injury. Sera samples are colored according to injury class where red, yellow, and green sera correspond to repeat injury, single injury, and sham serum samples. An X is drawn at the centroid of each class to indicate average scores on LVs 1 and 2 with the single impact centroids being displayed in black for visibility. Arrows are drawn at each timepoint to indicate centroid movement where the tail of the arrow corresponds to the centroid of the given class at baseline and the head points to the centroid of sera samples at the timepoint of blood collection.

4.3 Discriminant Metabolite Identification

Following multivariate analysis, feature identification was performed for the features in both final models and 19 of the 23 unique metabolites were identified using high resolution MS and MS/MS data (Table 2). Appendix A provides detailed MS/MS fragmentation information and the confidence level for each identified species. Most identified species were matched to inhouse or global database entries or matched to predicted spectra within Lipid Maps and HMDB databases. Metabolites in the panel

consisted of lipid species from the PC, SM, TG, PS, and ceramide lipid classes. Features without assignment could not be matched to MS/MS fragmentation spectra or to in house or publicly available databases and require further research for identification.

Table 2a: Annotation of lipids from the 16-feature male panel. Retention time, observed exact mass with instrumental error, observed adduct, predicted elemental formula, p-value of average abundance between sham and TBI, and fold change (FC) are reported. Positive FC values correspond to increased abundance in injured serum versus uninjured serum. Fatty acid chain information is included when MS/MS experiments were possible and detailed MS/MS fragmentation information provided in the appendix (Table A2).

Feature Number	RT (min)	<i>m/z</i> mass error (ppm)	Adduct	Elemental Formula	ID	p-value (TBI vs sham)	FC (TBI vs sham)
610	3.668	874.56116 1.578	[M+HCO ₂] ⁻	C ₄₈ H ₈₀ NO ₈ P	PC(20:4_20:4)	0.00113	1.719
1842	3.984	866.59186 0.902	[M-H] ⁻	C ₄₈ H ₈₆ NO ₁₀ P	PS(26:4_16:0)	0.000153	-1.531
2060	5.104	862.59662 0.529	[M+HCO ₂] ⁻	C ₄₉ H ₈₆ NO ₉ P	PC(O-18:1_22:6)	0.00974	1.505
3655	4.691	834.60156 0.373	[M+H] ⁺	C ₄₈ H ₈₄ NO ₈ P	PC(18:0_22:6)	0.000935	1.673
3961	3.605	830.56927 -0.818	[M+H] ⁺	C ₄₈ H ₈₀ NO ₈ P	PC(20:4_20:4) PC(18:2_22:6)	0.00372	1.548
3975	3.606	808.58563 0.0396	[M+H] ⁺	C ₄₆ H ₈₂ NO ₈ P	PC(18:1_20:4)	0.00360	1.552
4393	6.646	823.67926 -2.754	[M+H] ⁺	C ₅₃ H ₉₀ O ₆	TG(18:3_14:0_18:3)	0.0291	1.562
4890	7.723	999.74091 -1.996	[M+H] ⁺	C ₆₇ H ₉₈ O ₆	TG(20:4_22:6_22:6)	0.00618	1.860
5749	6.894	851.69769 -0.548	[M+Na] ⁺	C ₄₈ H ₉₇ N ₂ O ₆ P	SM(d43:1)	0.0451	1.672
5878	6.907	812.69806 0.189	[M+H] ⁺	C ₄₈ H ₉₃ NO ₈	HexCer(d18:1/24:0)	0.0326	1.781
6833	8.267	851.71075 -2.439	[M+H] ⁺	C ₅₅ H ₉₄ O ₆	TG(18:3_16:0_18:3)	0.0326	-1.731
7173	5.570	768.59076 0.104	[M+H] ⁺	C ₄₄ H ₈₂ NO ₇ P	PC(O-16:0_20:4)	0.0254	-1.699
7530	7.484	845.66339 -2.944	[M+H] ⁺	C ₅₅ H ₈₈ O ₆	TG(52:9)	0.0343	-1.622
7901	6.825	1243.02515	[M+Na] ⁺	not identified	not identified	0.00718	1.608
11257	7.329	846.75543 -0.479	[M+NH ₄] ⁺	C ₅₃ H ₉₆ O ₆	TG(16:0_16:1_18:2)	0.0490	1.545
13399	2.533	299.13901	not identified	not identified	not identified	0.000816	1.854

Table 2b: Annotation of lipids first from the 17-feature female panel. Retention time, observed exact mass with instrumental error, observed adduct, predicted elemental formula, p-value of average abundance between sham and TBI, and fold change (FC) are reported. Positive FC values correspond to increased abundance in injured serum versus uninjured serum. Fatty acid chain information is included when MS/MS experiments were possible and detailed MS/MS fragmentation information provided in the appendix (Table A2).

Feature Number	RT (min)	<i>m/z</i> mass error (ppm)	Adduct	Elemental Formula	ID	p-value (TBI vs. sham)	FC (TBI vs. sham)
610	3.668	874.56067 1.018	[M+HCO ₂] ⁻	C ₄₈ H ₈₀ NO ₈ P	PC(20:4_20:4)	0.00113	1.719
2060	5.104	862.59662 0.529	[M+HCO ₂] ⁻	C ₄₉ H ₈₆ NO ₉ P	PC(O-18:1_22:6)	0.00974	1.505
3655	4.691	834.60156 0.373	[M+H] ⁺	C ₄₈ H ₈₄ NO ₈ P	PC(18:0_22:6)	0.000935	1.673
3814	7.602	969.77856 -0.427	[M+NH ₄] ⁺	C ₆₃ H ₁₀₀ O ₆	TG(18:2_20:4_22:6)	0.0350	1.648
3961	3.605	830.56927 -0.818	[M+H] ⁺	C ₄₈ H ₈₀ NO ₈ P	PC(20:4_20:4) PC(18:2_22:6)	0.00372	1.548
3975	3.606	808.58563 0.0396	[M+H] ⁺	C ₄₆ H ₈₂ NO ₈ P	PC(18:1_20:4)	0.00360	1.552
4393	6.646	823.67926 -2.754	[M+H] ⁺	C ₅₃ H ₉₀ O ₆	TG(18:3_14:0_18:3)	0.0291	1.562
4499	8.180	972.80182 -0.155	[M+NH ₄] ⁺	C ₆₃ H ₁₀₂ O ₆	TG(18:0_20:4_22:6)	0.00721	1.911
4588	7.599	994.78564 -0.685	[M+NH ₄] ⁺	C ₆₅ H ₁₀₀ O ₆	TG(18:1_22:6_22:6)	0.0440	2.292
4890	7.723	999.74091 -1.996	[M+H] ⁺	C ₆₇ H ₉₈ O ₆	TG(20:4_22:6_22:6)	0.00618	1.860
5749	6.894	851.69769 -0.548	[M+Na] ⁺	C ₄₈ H ₉₇ N ₂ O ₆ P	SM(d43:1)	0.0451	1.672
5878	6.907	812.69806 0.189	[M+H] ⁺	C ₄₈ H ₉₃ NO ₈	HexCer(d18:1/24:0)	0.0326	1.781
6105	7.634	847.67889	not identified	not identified	not identified	0.0465	-1.764
6603	7.283	686.64246	not identified	not identified	not identified	0.0252	1.589
6698	3.362	878.56952 -0.488	[M+H] ⁺	C ₄₉ H ₇₄ NO ₈ P	PC(44:12)	0.0380	-1.581
7151	5.780	566.55096 -0.406	[M+H] ⁺	C ₃₆ H ₇₁ NO ₃	Cer(d18:1/18:0)	0.0435	2.093
7173	5.570	768.59076 0.104	[M+H] ⁺	C ₄₄ H ₈₂ NO ₇ P	PC(O-16:0_20:4)	0.0254	-1.699

4.4 TBI Lipidome Alterations

Discovering the biological role of specific metabolites and trends in lipid classes following TBI is critical to understanding the complexity and subtleties of TBI. The most identified classes of lipids from the final feature panels created in this study belonged to the PC and TG lipid classes with most species from both classes showing increased FC following injury. Increases in PC lipids have been documented in the CSF of severe TBI human patients in the hours and days following injury and recently have been reported in repeated closed skull CCI mice models in the cortex and hippocampus.^{118,165} A recent repetitive closed skull CCI injury study conducted by Ojo et al. found average PC lipid concentration in the brain to increase significantly, $p < 0.01$, at 24 h post-injury and return to levels similar to sham models by 3 months. Similar increases in serum PC species of repeat injury models discovered in this study warrant class investigation of PC as a potential indication of repeat injury. While TG lipid species have been far less researched regarding alterations following TBI recent work assessing post traumatic epilepsy, a common long-term risk associated with TBI, in rats has shown significant increases in TG concentration in the brain. Post traumatic epilepsy animals showed significant TG, $p < 0.005$, and PL, $p < 0.05$, increases beginning at 1 day and continuing as far as 30 days post epileptic seizure event.¹⁶⁶ Future investigation of TG as a class within the serum of TBI models present a unique opportunity for discovery especially if these finding can be linked to alterations in the brain.

Other features identified in the final optimized panels included a SM, PS, and several ceramide species. MSI experiments have identified ceramides to increase significantly surrounding the site of injury following CCI experiments as early as 24 h post

injury.¹⁶⁷ A 2016 study identified Cer(d18:1/18:0) to be significantly increased in the site surrounding CCI at one day, $p < 0.001$, and 7 days, $p < 0.01$, post-injury.¹⁶⁸ Similar increases in Cer(d18:1/18:0) found in the serum of injured animals in this study (Figure 7) may provide a useful link to understanding lipid species which increase directly at the site of injury and in peripheral serum biofluid. SM lipid species have also been reported to increase following CCI in as little as 4 h following injury.¹⁶⁹ The accumulation of SM species results from the stimulation of de novo biosynthesis of ceramide a precursor to SM. Minimal research has been conducted to investigate the alterations of PS species following TBI likely because of their low relative abundance in the brain. The single PS species identified in the final male optimized panel was found to significantly decrease at nearly all post-injury timepoints for male serum samples (Figure 7). While alterations were less significant in female serum samples similar trends were observed across all injury timepoints.

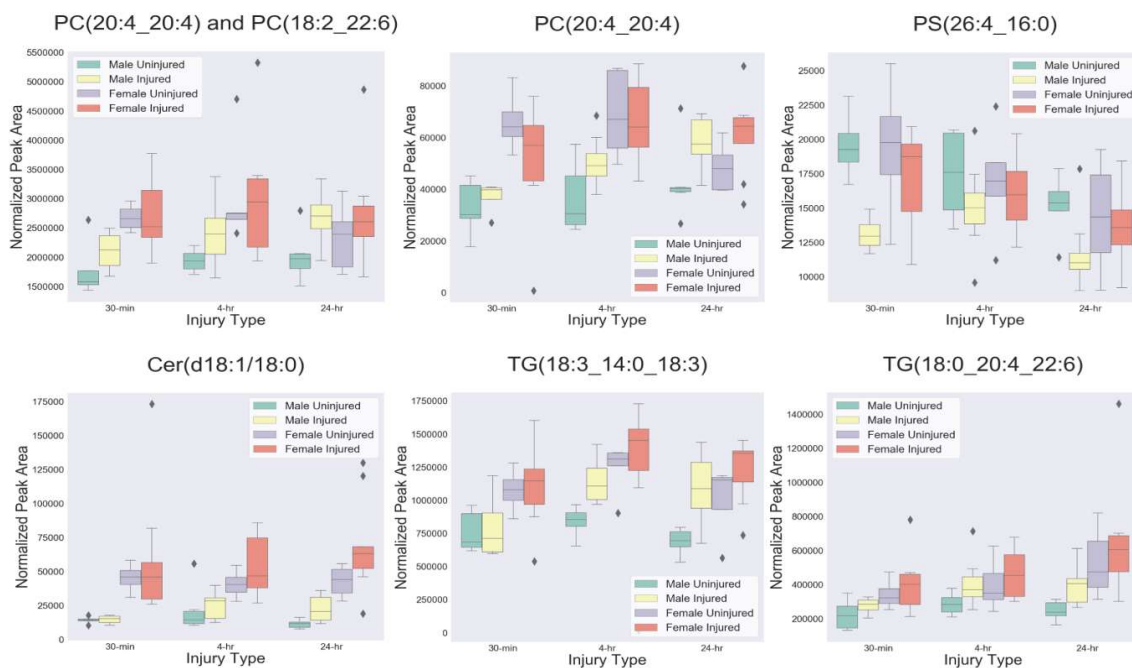


Figure 7: Box plots of selected features from the optimized feature panels to highlight alterations in identified lipid species across blood collection timepoints and sexes. Green and yellow boxplots correspond to male injured and uninjured serum samples respectively and purple and red colored boxplots correspond to uninjured and injured female serum samples, respectively. Black bars within each boxplot are used to show the median normalized area and outliers are drawn as black diamonds. Time point of blood collection is shown chronologically along the x-axis.

4.5 Conclusions

The research presented in this thesis shows the potential of lipids as biomarkers for TBI across a range of variables including acute post-injury timepoints, sex, and injury severity. Additional work is required to demonstrate the repeatability of the proposed biomarker candidates namely via orthopedic controls to evaluate whether these markers are specific to brain injury versus general inflammation. Increased frequency of blood collection at a greater number of acute post injury timepoints is needed to determine the optimal time at which these biomarker candidates should be tested for and to gauge recovery rates. While it is proposed that small non-polar lipid molecules can permeate the

BBB, this has only been definitively shown in higher severity injury models and while it is likely true to a similar or lesser extent for lower severity injuries further research is required to validate this claim. Measuring the alterations of the proposed serum biomarkers in the brain is crucial to understanding their influence on TBI pathophysiology. Similar LC-MS experiments on the homogenized cortex of the same rodent models used in this research will help guide future research toward connecting the blood and the brain. Additionally, spatial understanding of the features identified within this work is best investigated using MSI methodologies and is needed to enhance the qualitative and quantitative understanding of TBI directly at the site of injury and in surrounding brain regions.

APPENDIX A:

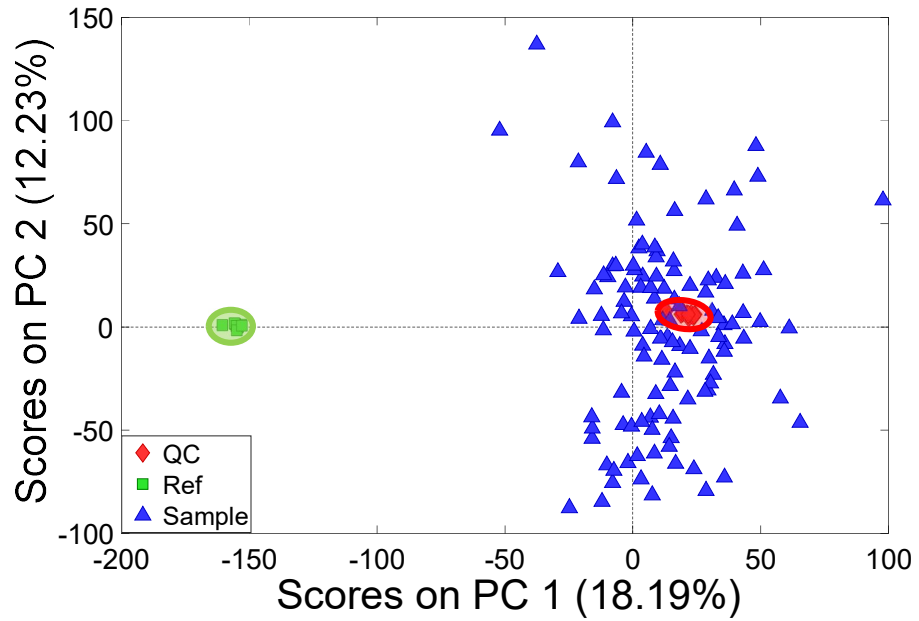


Figure A1: Unsupervised Principal Component Analysis score plot of all 14,119 features prior to feature selection. The distribution of samples shows clustering of quality control samples in the center of all study subject serum samples and separation of reference serum samples from study subject serum.

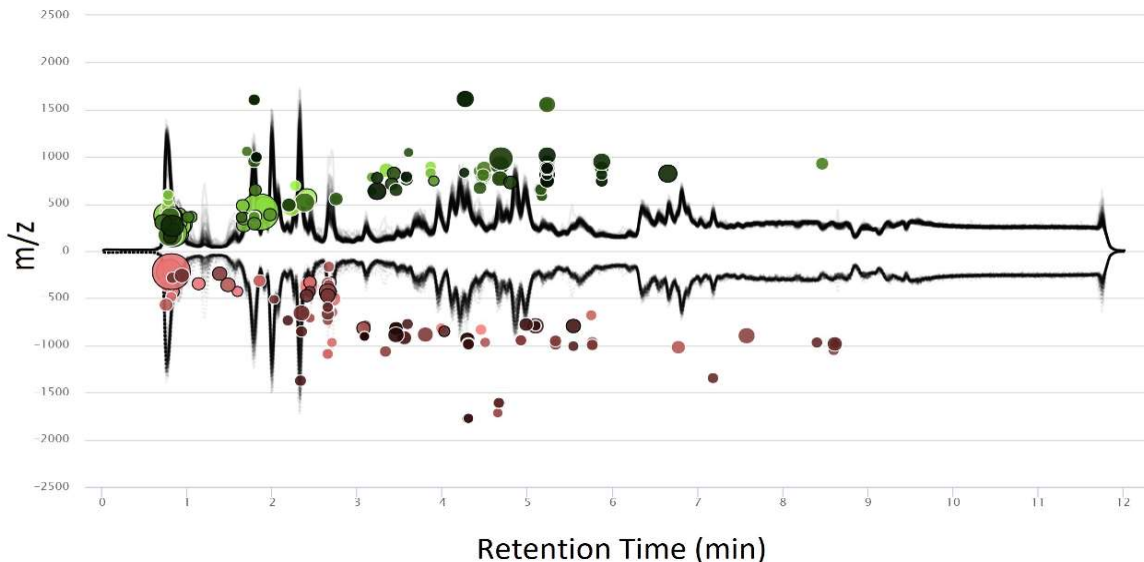


Figure A2: Cloud plot generated in the XCMS web-based application to portray all significantly differential features from negative mode MS data in injured (green) and uninjured (red) mTBI serum samples. The black traces outline chromatographic retention time on the x-axis and m/z values on the y-axis for each sample. Each bubble in the plot corresponds to one metabolite feature with fold change at or above 1.5 and a p-value at or below 0.05 using a Welsch's t-test. The color and size of each bubble denote the directionality and magnitude of fold change respectively with larger bubbles representing larger fold changes. The darkness of color in each bubble represents p-value significance with darker colors corresponding to features with greater statistical significance.

Table A1: Summary of GA variable selection parameters for both optimized feature panels

Population Size	64
Percent of Initial Terms Included	30
Window Width	1
Target Number Maximum Variables	30
Target Number Minimum Variables	10
Penalty Slope	0.05
Maximum Generations	200
Percent Convergence	50%
Mutation Rate	0.005
Regression Method	Partial Least Squares
Cross Validation	Random
Number of Cross Validation Data Splits	8
Number of Iterations of Cross Validation	10
Replicate Runs	5

Table A2: Detailed MS/MS information of all features selected in the male and female optimized panels separating injured and uninjured sera. Fragment ions were obtained using DDA experiments in either the positive or negative ion modes. Precursor ions selected for fragmentation are underlined and species matching either predicted spectra or standards are shown in bold. Confidence in metabolite identities is categorized by four levels 1) fragmentation pattern consistent with spectra from local or global databases and matched to predicted spectra from HMDB or LIPID Maps; 2) match to spectra in database but predicted fragmentation patterns not available; 3) match to predicted spectra but not matched to compounds in databases; 4) accurate mass match to Lipid Maps, HMDB or Metlin database entries; 5) unknown compound. ID's with confidence levels below 2 should be considered tentative until further research can be pursued.

Feature ID	CE (eV), Mode	Fragment Ion m/z	ID Confidence Level	Match Details (Source)
610	30 (-)	<u>874.56</u> , 814.61 , 528.24 , 327.19 , 303.25 , 279.16 224.10	1	Match to local database and match to predicted Lipid Maps spectra
1842	30 (-)	<u>866.59</u> , 806.67, 568.36 , 550.36 , 479.31, 255.20	4	Accurate mass match HMDB 16:0 fatty acyl chain (255) 18:2 and 22:6 (550 and 568)
2060	30 (-)	<u>842.59</u> , 782.70 774.59 , 464.40 , 327.26 , 283.34 , 195.85 , 139.91	2	Match to local database

Table A2 Continued

3655	35 (+)	<u>834.60</u>, 651.60, 550.43, 524.44, 506.47, 184.06, 125.04, 105.02	1	Match to local database and match to predicted HMBD spectrum
3814	30 (+)	<u>968.77</u>, 951.72, 933.80, 690.60, 671.39, 647.54, 623.54, 603.48, 385.30, 337.32, 311.20, 293.34, 287.26, 269.20, 245.05, 203.16, 157.18, 119.14	3	Match to predicted spectra in LIPID MAPS
3961	30 (+)	<u>830.57</u>, 812.84, 771.59, 762.80, 694.84, 647.70, 605.53, 568.51, 550.38, 544.54, 526.55, 502.26, 500.33, 184.11, 124.98	1	Match to local database and match to predicted HMBD spectrum

Table A2 Continued

3975	35 (+)	<u>808.59</u>, 790.61, 749.56, 625.57, 552.39, 522.46, 496.43, 478.42, 184.11, 124.98,	1	Match to local database and match to predicted HMDB spectrum
4393	30 (+)	<u>823.67</u>, 805.79, 687.90, 623.56, 597.50, 595.54, 569.51, 567.57, 545.52, 543.48, 541.55, 523.52, 301.12	1	Spectra match to Chem Spider Database and Lipid Maps predicted spectra
4499	30 (+)	<u>972.80</u>, 955.93, 904.80, 671.27, 651.62, 627.62, 602.55, 341.31, 287.27, 269.33, 203.12, 173.06, 119.09	3	Match to Lipid Maps predicted spectra

Table A2 Continued

4588	30 (+)	<u>994.78</u>, 977.79, 695.26, 649.59, 591.02, 430.23, 385.23, 339.33, 311.17, 269.23, 265.40, 249.25, 183.10, 145.06	3	Match to predicted spectra in Lipid Maps and HMBD
4890	35 (+)	<u>999.74</u>, 717.59, 695.54, 671.62, 669.57, 649.61, 351.31	1	Match to Chem Spider Database and LIPID MAPS predicted spectra
5749	30 (+)	<u>851.70</u>, 828.79, 805.89, 792.68, 783.79, 184.07	4	Accurate mass match HMBD
5878	30 (+)	<u>812.69</u>, 794.68, 632.63, 614.62, 368.39, 282.27, 264.27, 252.27	1	Accurate mass match Metlin and literature spectra

Table A2 Continued

6105	35 (+)	<u>847.68</u> , 762.74, 585.61, 580.50, 569.45, 549.45, 567.43, 543.19, 319.23, 238.14, 215.19, 135.14, 120.99	5	-
6603	30 (+)	<u>686.64</u> , 599.79, 550.81, 440.36, 370.32, 318.38, 257.18, 102.15	5	-
6698	30 (+)	<u>878.61</u> , 780.63, 695.56 , 601.50 , 575.51, 184.10 , 159.07, 173.46, 125.02	1	Match to local database and match to predicted HMDB spectrum
6833	30 (+)	<u>851.71</u> , 623.63, 597.60, 595.57 , 573.57 , 571.53, 569.57, 549.57, 303.29	1	Match to Chem Spider Database and Lipid Maps predicted spectra

Table A2 Continued

7151	30 (+)	<u>566.55</u> , <u>548.54</u> , <u>530.53</u> , 289.89, <u>282.28</u> , <u>264.27</u> , 252.27, 173.45	3	Fragmentation consistent with predicted HMBD spectra
7173	30 (+)	<u>768.59</u> , <u>750.73</u> , 727.51, <u>724.61</u> , 722.84, <u>682.59</u> , 632.94, <u>627.64</u> , 467.41, 369.40, <u>283.16</u> , 282.30, <u>184.11</u> , <u>125.05</u> , <u>88.11</u>	1	Match to local database and match to predicted HMBD spectrum
7530	35 (+)	<u>845.66</u> , 814.61, 792.49, 777.78, 763.53, 709.88, 641.79, 597.50, 573.75, 565.52, 455.68, 437.60, 226.96	4	Accurate mass match (HMBD)
7901	35 (+)	<u>1243.03</u> , 1197.15, 1187.98, 623.92	5	-

Table A2 Continued

11257	30 (+)	846.75, 829.85, 811.80, 601.64, 757.61, 573.73, 549.59, 547.47, 313.27, 263.24, 135.12, 95.09	1	Match to local database and match to predicted HMBD spectrum
13399	30 (+)	<u>299.14,</u> 281,22, 257.17, 239.18	5	-

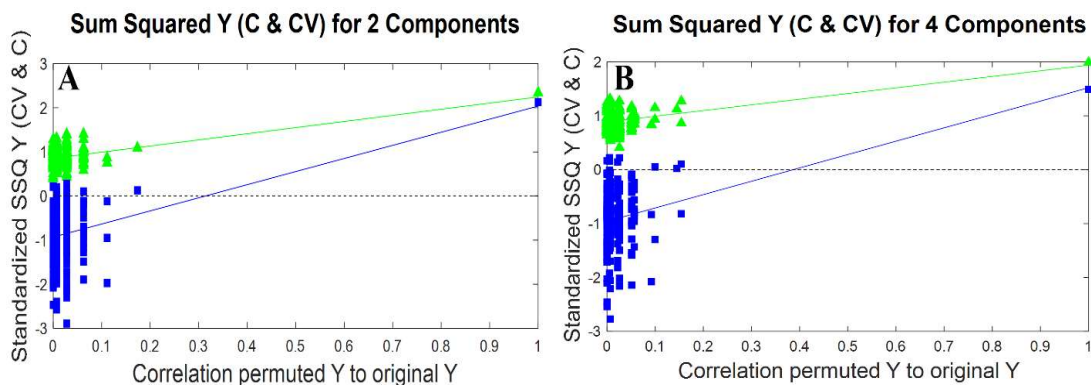


Figure A3: Permutation test results for the male (A) and female (B) optimized panels to evaluate over fitness. Random reordering of class assignments over 200 iterations provided nominally incorrect class assignments to the data and attempted to build models using the same set of features with randomly assigned classes. This method examines the extent to which the models are finding chance correlations between the data and class assignments are and overfit to the given data. In general, the cross-validated results shown in blue are relatively close to the self-predicted results shown in green and permuted results shown on the left are far from the un-permuted original model shown on the far right indicating a strong lack of over fitness. The non-permuted results on the far right are more than several standard deviations from the bulk of the corresponding permuted results indicating a lack of over fitting.

Table A3: Results of permutation testing on the self-predicted residuals and the cross-validated residuals obtained when a model is built from a subset of the data. Results are reported as a probability that the original model is indistinguishable from models created using randomly shuffled class assignments. The results from Wilcoxon, sign-tests, and random t-tests are shown and all indicate that the model is very unlikely to be random at the $\alpha = 0.005$ confidence limit.

Male 2 LV's			
Method	Wilcoxon	Sign Test	Rand t-test
Self-Prediction	0.000	0.002	0.005
Cross Validated	0.000	0.000	0.005
Female 4 LV's			
Method	Wilcoxon	Sign Test	Rand t-test
Self-Prediction	0.000	0.001	0.005
Cross Validated	0.000	0.001	0.005

REFERENCES

- (1) Gregory L. Goodrich, H. M. F.; Kirby, J. E.; Chang, C.-Y.; Martinsen, and G. L. M. Mechanisms of TBI and Visual Consequences In. **2013**, *90* (2), 105–112.
- (2) Asarnow, T. B. and R. Neurocognitive Outcomes and Recovery After Pediatric TBI: Meta-Analytic Review of the Literature. **2014**, *23* (3), 283–296. <https://doi.org/10.1037/a0015268>. Neurocognitive.
- (3) Jordan, B. D. The Clinical Spectrum of Sport-Related Traumatic Brain Injury. *Nat. Rev. Neurol.* **2013**, *9* (4), 222–230. <https://doi.org/10.1038/nrneuro.2013.33>.
- (4) Biswas, R. K.; Kabir, E.; King, R. Effect of Sex and Age on Traumatic Brain Injury: A Geographical Comparative Study. *Arch. Public Heal.* **2017**, *75* (1), 1–11. <https://doi.org/10.1186/s13690-017-0211-y>.
- (5) Fehily, B.; Fitzgerald, M. Repeated Mild Traumatic Brain Injury: Potential Mechanisms of Damage. *Cell Transplant.* **2017**, *26* (7), 1131–1155. <https://doi.org/10.1177/0963689717714092>.
- (6) Stein, D. G. Embracing Failure: What the Phase III Progesterone Studies Can Teach about TBI Clinical Trials. *Brain Inj.* **2015**, *29* (11), 1259–1272. <https://doi.org/10.3109/02699052.2015.1065344>.
- (7) Dewan, M. C.; Rattani, A.; Gupta, S.; Baticulon, R. E.; Hung, Y. C.; Punchak, M.; Agrawal, A.; Adeleye, A. O.; Shrimel, M. G.; Rubiano, A. M.; Rosenfeld, J. V.; Park, K. B. Estimating the Global Incidence of Traumatic Brain Injury. *J. Neurosurg.* **2019**, *130* (4), 1080–1097. <https://doi.org/10.3171/2017.10.JNS17352>.
- (8) Barnes, D. E.; Byers, A. L.; Gardner, R. C.; Seal, K. H.; Boscardin, W. J.; Yaffe, K. Association of Mild Traumatic Brain Injury with and without Loss of Consciousness with Dementia in US Military Veterans. *JAMA Neurol.* **2018**, *75* (9), 1055–1061. <https://doi.org/10.1001/jamaneurol.2018.0815>.
- (9) Saatian, M. R.; Ahmadpoor, J.; Mohamadi, Y.; Mazloumi, E. Epidemiology and Pattern of Traumatic Brain Injury in a Developing Country Regional Trauma Center. *Bull. Emerg. Trauma* **2018**, *6* (1 JAN), 45–53. <https://doi.org/10.29252/beat-060107>.
- (10) Peterson, A. Surveillance Report of Traumatic Brain Injury-Related Emergency Department Visits, Hospitalizations, and Deaths-United States, 2014. *Centers Dis. Control Prev. U.S. Dep. Heal. Hum. Serv.* **2019**, *24*.
- (11) Hilaire J. Thompson, Wayne C. McCormick, and S. H. K. Traumatic Brain Injury in Older Adults: Epidemiology, Outcomes, and Future Implications. *J Am Geriatr Soc* **2012**, *54* (10), 1590–1595.
- (12) Taylor, C.; Bell, J. M.; Breiding, M. J.; Xu, L. Traumatic Brain Injury-Related Emergency Department Visits, Hospitalizations, and Deaths-United States, 2007 and 2013 Surveillance Summaries Centers for Disease Control and Prevention MMWR Editorial and Production Sta. *Morb. Mortal. Wkly. Rep.* **2017**, *66* (9), 1–8.
- (13) Faul, M.; Coronado, V. *Epidemiology of Traumatic Brain Injury*, 1st ed.; Elsevier B.V., 2015; Vol. 127. <https://doi.org/10.1016/B978-0-444-52892-6.00001-5>.
- (14) Daneshvar, D. H.; Nowinski, C. J.; Mckee, A. C.; Cantu, R. C. The Epidemiology of Sport-Related Concussion. *Clin. Sports Med.* **2011**, *30* (1), 1–17.

- <https://doi.org/10.1016/j.csm.2010.08.006>.
- (15) Ryu, W. H. A.; Feinstein, A.; Colantonio, A.; Streiner, D. L.; Dawson, D. R. Early Identification and Incidence of Mild TBI in Ontario. *Can. J. Neurol. Sci.* **2009**, *36* (4), 429–435. <https://doi.org/10.1017/S0317167100007745>.
 - (16) Gouvier, W. D.; Uddo-Crane, M.; Brown, L. M. Base Rates of Post-Concussional Symptoms. *Arch. Clin. Neuropsychol.* **1988**, *3* (3), 273–278. [https://doi.org/10.1016/0887-6177\(88\)90019-4](https://doi.org/10.1016/0887-6177(88)90019-4).
 - (17) Wäljas, M.; Iverson, G. L.; Lange, R. T.; Hakulinen, U.; Dastidar, P.; Huhtala, H.; Liimatainen, S.; Hartikainen, K.; Öhman, J. A Prospective Biopsychosocial Study of the Persistent Post-Concussion Symptoms Following Mild Traumatic Brain Injury. *J. Neurotrauma* **2015**, *32* (8), 534–547. <https://doi.org/10.1089/neu.2014.3339>.
 - (18) Fu, T. S.; Jing, R.; McFaull, S. R.; Cusimano, M. D. Health & Economic Burden of Traumatic Brain Injury in the Emergency Department. *Can. J. Neurol. Sci.* **2015**, *43* (2), 238–247. <https://doi.org/10.1017/cjn.2015.320>.
 - (19) Wehrmacher, W. H.; Messmore, H.; Messmore, H. L.; Cukierman, S. Applied Epidemiology. Theory to Practice, 2nd Edition. *Compr. Ther.* **2007**, *33* (3), 164–165. <https://doi.org/10.1007/s12019-007-0018-9>.
 - (20) Brain, T.; Page, I.; Resources, G.; Brochures, O.; Act, R.; Information, F.; Diversity, E.; People, F. Traumatic Brain Injury : Hope Through Research. **2013**.
 - (21) Huff, J. G. J. S. *Closed Head Trauma*.; StatPearls Publishing: Treasure Island (FL), 2020.
 - (22) Bodnar, C. N.; Roberts, K. N.; Higgins, E. K.; Bachstetter, A. D. A Systematic Review of Closed Head Injury Models of Mild Traumatic Brain Injury in Mice and Rats. *J. Neurotrauma* **2019**, *36* (11), 1683–1706. <https://doi.org/10.1089/neu.2018.6127>.
 - (23) Werner, C.; Engelhard, K. Pathophysiology of Traumatic Brain Injury. *Br. J. Anaesth.* **2007**, *99* (1), 4–9. <https://doi.org/10.1093/bja/aem131>.
 - (24) Drew, L. B.; Drew, W. E. New Perspectives in Brain Injury The Contrecoup–Coup Phenomenon A New Understanding of the Mechanism of Closed Head Injury. *Neurocrit. Care* **2004**, 385–390.
 - (25) Marshall, L. F. Principal ' S Editorial. **2000**, *47* (3).
 - (26) Osier, N.; Dixon, C. E. Mini Review of Controlled Cortical Impact: A Well-Suited Device for Concussion Research. *Brain Sci.* **2017**, *7* (7). <https://doi.org/10.3390/brainsci7070088>.
 - (27) Hilaire J. Thompson, Jonathan Lifshitz, Niklas Marklund, M. Sean Grady, David I. Graham, David A. Hovda, and T. K. M. Lateral Fluid Percussion Brain Injury: A 15-Year Review and Evaluation. *J. Neurotrauma* **2005**, *22* (1), 42–75.
 - (28) Andriessen, T. M. J. C.; Jacobs, B.; Vos, P. E. Clinical Characteristics and Pathophysiological Mechanisms of Focal and Diffuse Traumatic Brain Injury. *J. Cell. Mol. Med.* **2010**, *14* (10), 2381–2392. <https://doi.org/10.1111/j.1582-4934.2010.01164.x>.
 - (29) Mishra, V.; Skotak, M.; Schuetz, H.; Heller, A.; Haorah, J.; Chandra, N. Primary Blast Causes Mild, Moderate, Severe and Lethal TBI with Increasing Blast Overpressures: Experimental Rat Injury Model. *Sci. Rep.* **2016**, *6* (April), 1–14. <https://doi.org/10.1038/srep26992>.

- (30) Mackenzie, J. A.; McMillan, T. M. Knowledge of Post-Concussional Syndrome in Naïve Lay-People, General Practitioners and People with Minor Traumatic Brain Injury. *Br. J. Clin. Psychol.* **2005**, *44* (3), 417–424. <https://doi.org/10.1348/014466505X35696>.
- (31) O’Neil, M. E. Complications of MTBI in Veterans and Military Personnel: A Systematic Review. *Heal. Serv. Research Dev. Serv.* **2013**.
- (32) Maskell, F.; Chiarelli, P.; Isles, R. Dizziness after Traumatic Brain Injury: Overview and Measurement in the Clinical Setting. *Brain Inj.* **2006**, *20* (3), 293–305. <https://doi.org/10.1080/02699050500488041>.
- (33) Teasdale Jennett, G. B. ASSESSMENT OF COMA AND IMPAIRED CONSCIOUSNESS: A Practical Scale. *Lancet* **1974**, *304* (7872), 81–84.
- (34) Sternbach, G. The Glasgow Coma Scale. *Med. Class.* **2000**, *19* (1), 67–71.
- (35) Grote, S.; Mutschler, W. Diagnostic Value of the Glasgow Coma Scale for Traumatic Brain Injury in 18 , 002 Patients with Severe Multiple Injuries. **2011**, *534* (April), 527–534. <https://doi.org/10.1089/neu.2010.1433>.
- (36) Stuke, L.; Diaz-arrastia, R.; Gentilello, L. M. Effect of Alcohol on Glasgow Coma Scale In. **2007**, *245* (4), 651–655. <https://doi.org/10.1097/01.sla.0000250413.41265.d3>.
- (37) Digiorio, A. M.; Wittenberg, B. A.; Ii, C. L. C.; Kennamer, B.; Greene, C. S.; Velandar, A. J.; Wilson, J. D.; Tender, G. C.; Culicchia, F.; Hunt, J. P. The Impact of Drug and Alcohol Intoxication on Glasgow Coma Scale Assessment in Patients with Traumatic Brain Injury. *World Neurosurg.* **2020**, *135*, e664–e670. <https://doi.org/10.1016/j.wneu.2019.12.095>.
- (38) Segatore M, W. C. The Glasgow Coma Scale: Time for Change. *J. Crit. Care* **1992**, *6*, 548–557.
- (39) Rohaut, B.; Porcher, R.; Hissem, T.; Heming, N.; Chillet, P.; Djedaini, K.; Moneger, G.; Kandelman, S.; Allary, J.; Antona, M.; Azabou, E.; Cariou, A.; Sonnevile, R.; Annane, D.; Siami, S.; Chre, F. Brainstem Response Patterns in Deeply- Sedated Critically-Ill Patients Predict 28-Day Mortality. *PLoS One* **2017**, 1–17.
- (40) STANCZAK, DANIEL WHITE III, J.; GOUVIEW, WILLIAM MOEHLE, KURT DANIEL, M.; NOVACK, THOMAS LONG, C. Assessment of Level of Consciousness Following Severe Neurological Insult. *J Neurosurg* **1984**, *60*, 955–960.
- (41) Kwang, S.; Joo, H.; Park, H. Clinical Efficacy of the Romberg Test Using a Foam Pad to Identify Balance Problems : A Comparative Study with the Sensory Organization Test. *Eur. Arch. Oto-Rhino-Laryngology* **2015**, *272* (10), 2741–2747. <https://doi.org/10.1007/s00405-014-3273-2>.
- (42) Wade, L. D.; Canning, C. G.; Fowler, V.; Felmingham, K. L.; Bag, I. J.; Ld, W.; Cc, C.; Fowler, V. Changes in Postural Sway and Performance of Functional Tasks During Rehabilitation After Traumatic Brain Injury. **1997**, *78* (October).
- (43) Berg, K.; Wood-Dauphinee, S.; Williams, I.; Maki, B. Measuring Balance in the Elderly : Validation of an Instrument. *Can. J. Public Heal.* **1992**, *83* (Suppl), 7–11.
- (44) Pickett, T. C.; Radfar-baublitz, L. S.; Mcdonald, S. D.; Walker, W. C.; Cifu, D. X. Objectively Assessing Balance Deficits after TBI: Role of Computerized Posturography. **2007**, *44* (7), 983–990.

- <https://doi.org/10.1682/JRRD.2007.01.0001>.
- (45) Guskiewicz, K. M.; Weaver, N. L.; Padua, D. A.; Garrett, W. E.; Hill, C.; Carolina, N. Epidemiology of Concussion in Collegiate and High School Football Players. **2000**, *28* (5).
 - (46) Guskiewicz, K. M. Balance Assessment in the Management of Sport-Related Concussion. *Clin. Sports Med.* **2011**, *30* (1), 89–102. <https://doi.org/10.1016/j.csm.2010.09.004>.
 - (47) Johnston, W.; Coughlan, G. F.; Caulfield, B. Challenging Concussed Athletes : The Future of Balance Assessment in Concussion. **2017**, No. December 2016, 779–783. <https://doi.org/10.1093/qjmed/hcw228>.
 - (48) Scores, S.; Athletes, D. F.; Mathiasen, R.; Hogrefe, C.; Harland, K.; Peterson, A.; Smoot, M. K. Longitudinal Improvement in Balance Error Scoring. **2018**, *694*, 691–694. <https://doi.org/10.1089/neu.2017.5072>.
 - (49) Wilkins, J. C.; Mcleod, T. C. V.; Perrin, D. H.; Gansneder, B. M. System Decreases After Fatigue. **2004**, *39* (2), 156–161.
 - (50) Teel, E. F.; Register-mihalik, J. K.; Blackburn, J. T.; Guskiewicz, K. M. Journal of Science and Medicine in Sport Balance and Cognitive Performance during a Dual-Task : Preliminary Implications for Use in Concussion Assessment. *J. Sci. Med. Sport* **2013**, *16* (3), 190–194. <https://doi.org/10.1016/j.jsams.2012.09.007>.
 - (51) Broglio, S. P.; Tomporowski, P. D.; Ferrara, M. S. Balance Performance with a Cognitive Task : A Dual-Task Testing Paradigm ABSTRACT. **2019**, No. April 2005. <https://doi.org/10.1249/01.MSS.0000159019.14919.09>.
 - (52) Scheibel, R. S.; Christiansen, C. H.; Huddleston, N.; Ottenbacher, K. J. Virtual Reality in the Assessment of Selected Cognitive Function After Brain Injury. **2001**, No. August, 597–604.
 - (53) Zhang, L.; Abreu, B. C.; Seale, G. S.; Masel, B.; Christiansen, C. H.; Ottenbacher, K. J.; L, A. Z.; Bc, A.; Gs, S.; Masel, B. A Virtual Reality Environment for Evaluation of a Daily Living Skill in Brain Injury Rehabilitation : Reliability and Validity. **2003**, *84* (August), 1118–1124. [https://doi.org/10.1016/S0003-9993\(03\)00203-X](https://doi.org/10.1016/S0003-9993(03)00203-X).
 - (54) Howell, D. R.; Osternig, L. R.; Chou, L. Return to Activity after Concussion Affects. **2015**, 673–680. <https://doi.org/10.1249/MSS.0000000000000462>.
 - (55) Fait, P.; Swaine, B.; Leblond, J.; Mcfadyen, B. J. Altered Integrated Locomotor and Cognitive Function in Elite Athletes 30 Days Postconcussion : A Preliminary Study. **2012**, No. April. <https://doi.org/10.1097/HTR.0b013e3182407ace>.
 - (56) Negrete, T. N.; Sosnoff, J. J.; Broglio, S. P.; Dn, A. M.; Mj, S.; Sa, D.; Ew, L. The Chronic Effects of Concussion on Gait. *YAPMR* **2011**, *92* (4), 585–589. <https://doi.org/10.1016/j.apmr.2010.11.029>.
 - (57) Tong, W. S.; Zheng, P.; Xu, J. F.; Guo, Y. J.; Zeng, J. S.; Yang, W. J.; Li, G. Y.; He, B.; Yu, H. Early CT Signs of Progressive Hemorrhagic Injury Following Acute Traumatic Brain Injury. *Neuroradiology* **2011**, *53* (5), 305–309. <https://doi.org/10.1007/s00234-010-0659-8>.
 - (58) Paulano, F.; Jiménez, J. J.; Pulido, R. 3D Segmentation and Labeling of Fractured Bone from CT Images. *Vis. Comput.* **2014**, *30* (6–8), 939–948. <https://doi.org/10.1007/s00371-014-0963-0>.
 - (59) Belanger, H. G.; Vanderploeg, R. D.; Curtiss, G.; Warden, D. L. Recent

- Neuroimaging Techniques in Mild Traumatic Brain Injury. *J. Neuropsychiatry Clin. Neurosci.* **2007**, *19* (1), 5–20. <https://doi.org/10.1176/jnp.2007.19.1.5>.
- (60) Shin, S. S.; Bales, J. W.; Edward Dixon, C.; Hwang, M. Structural Imaging of Mild Traumatic Brain Injury May Not Be Enough: Overview of Functional and Metabolic Imaging of Mild Traumatic Brain Injury. *Brain Imaging Behav.* **2017**, *11* (2), 591–610. <https://doi.org/10.1007/s11682-017-9684-0>.
- (61) Bergsneider, M.; Hovda, D. A.; Shalmon, E.; Kelly, D. F.; Vespa, P. M.; Martin, N. A.; Phelps, M. E.; McArthur, D. L.; Caron, M. J.; Kraus, J. F.; Becker, D. P. Cerebral Hyperglycolysis Following Severe Traumatic Brain Injury in Humans: A Positron Emission Tomography Study. *J. Neurosurg.* **1997**, *86* (2), 241–251. <https://doi.org/10.3171/jns.1997.86.2.0241>.
- (62) Buxton, R. B.; Uludağ, K.; Dubowitz, D. J.; Liu, T. T. Modeling the Hemodynamic Response to Brain Activation. *Neuroimage* **2004**, *23* (SUPPL. 1), 220–233. <https://doi.org/10.1016/j.neuroimage.2004.07.013>.
- (63) Provenzano, F. A.; Jordan, B.; Tikofsky, R. S.; Saxena, C.; Van Heertum, R. L.; Ichise, M. F-18 FDG PET Imaging of Chronic Traumatic Brain Injury in Boxers. *Nucl. Med. Commun.* **2010**, *31* (11), 952–957. <https://doi.org/10.1097/MNM.0b013e32833e37c4>.
- (64) McAllister, T. W.; Saykin, A. J.; Flashman, L. A.; Sparling, M. B.; Johnson, S. C.; Guerin, S. J.; Mamourian, A. C.; Weaver, J. B.; Yanofsky, N. Brain Activation during Working Memory 1 Month after Mild Traumatic Brain Injury: A Functional MRI Study. *Neurology* **1999**, *53* (6), 1300–1300. <https://doi.org/10.1212/WNL.53.6.1300>.
- (65) Avila-rodriguez, M. F.; Thelin, E. P. Monitoring the Neuroinflammatory Response Following Acute Brain Injury. **2017**, *8* (July), 1–14. <https://doi.org/10.3389/fneur.2017.00351>.
- (66) Prasetyo, E. The Primary , Secondary , and Tertiary Brain Injury. **2020**, 4–13.
- (67) Cicerone, K. D. Disturbance of Social Cognition Brain Injury After Traumatic Orbitofrontal. **1997**, *12* (2), 173–188.
- (68) Mcintosh, T. K.; Saatman, K. E.; Raghupathi, R.; Graham, D. I.; Smith, D. H.; Lee, V. M. The Dorothy Russell Memorial Lecture * The Molecular and Cellular Sequelae of Experimental Traumatic Brain Injury : Pathogenetic Mechanisms. **1998**, 251–267.
- (69) Bisri, D. Y. Serum Interleukin-6 Level after Cyclooxygenase-2 Inhibitor Treatment in Journal of Anesthesia & Clinical Serum Interleukin-6 Level after Cyclooxygenase-2 Inhibitor Treatment in Moderate Traumatic Brain Injury. **2017**, No. July 2018, 6–12. <https://doi.org/10.4172/2155-6148.1000711>.
- (70) Weber, J. T. Altered Calcium Signaling Following Traumatic Brain Injury. **2012**, *3* (April), 1–16. <https://doi.org/10.3389/fphar.2012.00060>.
- (71) Mattson, M. P. Calcium and Neurodegeneration. *Aging Cell* **2007**, No. 6, 337–350. <https://doi.org/10.1111/j.1474-9726.2007.00275.x>.
- (72) Bai, W.; Zhu, W.; Ning, Y.; Li, P.; Zhao, Y.; Yang, N.; Chen, X.; Jiang, Y.; Yang, W.; Jiang, D.; Chen, L.; Zhou, Y. Dramatic Increases in Blood Glutamate Concentrations Are Closely Related to Traumatic Brain Injury-Induced Acute Lung Injury. *Nat. Sci. Reports* **2017**, No. 7, 1–9. <https://doi.org/10.1038/s41598-017-05574-9>.

- (73) Roukoz, C.; Dima, S.; Gopinath, S.; Goodman, C.; Robertson, C. Role of Extracellular Glutamate Measured by Cerebral Microdialysis in Severe Traumatic Brain Injury. *J Neurosurg* **2010**, *113* (3), 564–570. <https://doi.org/10.3171/2009.12.JNS09689>.
- (74) Zamzami, N.; Hirsch, T.; Dallaporta, B.; Petit, P. X.; Kroemer, G. Mitochondrial Implication in Accidental and Programmed Cell Death : Apoptosis and Necrosis. *J. Bioenerg. Biomembr.* **1997**, *29* (2), 185–193.
- (75) Fink, S. L.; Cookson, B. T. Apoptosis , Pyroptosis , and Necrosis : Mechanistic Description of Dead and Dying Eukaryotic Cells. *Infect. Immun.* **2005**, *73* (4), 1907–1916. <https://doi.org/10.1128/IAI.73.4.1907>.
- (76) Higashida, T.; Kreipke, C.; Rafols, J.; Peng, C.; Schafer, S.; Schafer, P.; Veterans, J. D. D. The Role of Hypoxia-Inducible Factor-1 α , Aquaporin-4, and Matrix Metalloproteinase-9 in Blood-Brain Barrier Disruption and Brain Edema after Traumatic Brain Injury. *J Neurosurg* **2011**, *114* (January), 92–101. <https://doi.org/10.3171/2010.6.JNS10207>.
- (77) Lighthall, J. Controlled Cortical Impact: A New Experimental Brain Injury Model. *J. Neurotrauma* **1988**, *5* (1), 1–5.
- (78) Dixon, E.; Clifton, G.; Lighthall, J.; Yaghmai, A.; Hayes, R. A Controlled Cortical Impact Model of Traumatic Brain Injury in the Rat. *J. Neurosci. Methods* **1991**, *39* (3), 253–262.
- (79) Hamm, R.; Dixon, E.; Gbadebo, D.; Singha, A.; Jenkins, L.; Lyeth, B.; Hayes, R. Cognitive Deficits Following Traumatic Brain Injury Produced by Controlled Cortical Impact. *J. Neurotrauma* **1992**, *9* (1), 11–20.
- (80) Pham, L.; Shultz, S. R.; Kim, H. A.; Brady, R. D.; Wortman, R. C.; Genders, S. G.; Hale, M. W.; O’Shea, R. D.; Djouma, E.; Van Den Buuse, M.; Church, J. E.; Christie, B. R.; Drummond, G. R.; Sobey, C. G.; McDonald, S. J. Mild Closed-Head Injury in Conscious Rats Causes Transient Neurobehavioral and Glial Disturbances: A Novel Experimental Model of Concussion. *J. Neurotrauma* **2019**, *36* (14), 2260–2271. <https://doi.org/10.1089/neu.2018.6169>.
- (81) Chen, S.; Pickard, J. D.; Harris, N. G. Time Course of Cellular Pathology after Controlled Cortical Impact Injury. *Exp. Neurol.* **2003**, *182* (1), 87–102. [https://doi.org/10.1016/S0014-4886\(03\)00002-5](https://doi.org/10.1016/S0014-4886(03)00002-5).
- (82) Yu, S.; Kaneko, Y.; Bae, E.; Stahl, C. E.; Wang, Y.; van Loveren, H.; Sanberg, P. R.; Borlongan, C. V. Severity of Controlled Cortical Impact Traumatic Brain Injury in Rats and Mice Dictates Degree of Behavioral Deficits. *Brain Res.* **2009**, *1287*, 157–163. <https://doi.org/10.1016/j.brainres.2009.06.067>.
- (83) Ommaya, A.; Rockoff, D.; Baldwin, M.; Friauf, W. Experimental Concussion. *J. Neurosurg.* **1945**, *2*, 26–35.
- (84) Prins, M.; Greco, T.; Alexander, D.; Giza, C. C. The Pathophysiology of Traumatic Brain Injury at a Glance. *DMM Dis. Model. Mech.* **2013**. <https://doi.org/10.1242/dmm.011585>.
- (85) Flierl, M. A.; Stahel, P. F.; Beauchamp, K. M.; Morgan, S. J.; Smith, W. R.; Shohami, E. Mouse Closed Head Injury Model Induced by a Weight-Drop Device. *Nat. Protoc.* **2009**, *4* (9), 1328–1337. <https://doi.org/10.1038/nprot.2009.148>.
- (86) Bliven, E.; Rouhier, A.; Tsai, S.; Willinger, R.; Bourdet, N.; Deck, C.; Madey, S. M.; Bottlang, M. Evaluation of a Novel Bicycle Helmet Concept in Oblique

- Impact Testing. *Accid. Anal. Prev.* **2019**, *124* (November 2018), 58–65.
<https://doi.org/10.1016/j.aap.2018.12.017>.
- (87) Kane, M. J.; Angoa-Pérez, M.; Briggs, D. I.; Viano, D. C.; Kreipke, C. W.; Kuhn, D. M. A Mouse Model of Human Repetitive Mild Traumatic Brain Injury. *J. Neurosci. Methods* **2012**, *203* (1), 41–49.
<https://doi.org/10.1016/j.jneumeth.2011.09.003>.
- (88) Ning, Y. L.; Zhou, Y. G. Shock Tubes and Blast Injury Modeling. *Chinese J. Traumatol. - English Ed.* **2015**, *18* (4), 187–193.
<https://doi.org/10.1016/j.cjtee.2015.04.005>.
- (89) Panzer, M. B.; Matthews, K. A.; Yu, A. W.; Morrison, B.; Meaney, D. F.; Bass, C. R. A Multiscale Approach to Blast Neurotrauma Modeling: Part I - Development of Novel Test Devices for in Vivo and in Vitro Blast Injury Models. *Front. Neurol.* **2012**, *MAR* (March), 1–11. <https://doi.org/10.3389/fneur.2012.00046>.
- (90) Barnard, E.; Johnston, A. Blast Lung. *N. Engl. J. Med.* **2013**, *368* (11), 1045–1045.
<https://doi.org/10.1056/nejmicm1203842>.
- (91) Dadas, A.; Washington, J.; Diaz-arrastia, R.; Janigro, D. Ndt-14-2989.Pdf. **2018**, 2989–3000.
- (92) Wang, K. K.; Yang, Z.; Zhu, T.; Shi, Y.; Rubenstein, R.; Tyndall, J. A.; Manley, G. T. An Update on Diagnostic and Prognostic Biomarkers for Traumatic Brain Injury. *Expert Rev. Mol. Diagn.* **2018**, *18* (2), 165–180.
<https://doi.org/10.1080/14737159.2018.1428089>.
- (93) Czeiter, E.; Mondello, S.; Kovacs, N.; Sandor, J.; Gabrielli, A.; Schmid, K.; Tortella, F.; Wang, K. K. W.; Hayes, R. L.; Barzo, P.; Ezer, E.; Doczi, T.; Buki, A. Brain Injury Biomarkers May Improve the Predictive Power of the IMPACT Outcome Calculator. *J. Neurotrauma* **2012**, *29* (9), 1770–1778.
<https://doi.org/10.1089/neu.2011.2127>.
- (94) Middeldorp, J.; Hol, E. M. GFAP in Health and Disease. *Prog. Neurobiol.* **2011**, *93* (3), 421–443. <https://doi.org/10.1016/j.pneurobio.2011.01.005>.
- (95) Mondello, S.; Papa, L.; Buki, A.; Bullock, M. R.; Czeiter, E.; Tortella, F. C.; Wang, K. K.; Hayes, R. L. Neuronal and Glial Markers Are Differently Associated with Computed Tomography Findings and Outcome in Patients with Severe Traumatic Brain Injury : A Case Control Study. **2011**.
- (96) Papa, L.; Silvestri, S.; Brophy, G. M.; Giordano, P.; Falk, J. L.; Braga, C. F.; Tan, C. N.; Ameli, N. J.; Demery, J. A.; Dixit, N. K.; Mendes, M. E.; Hayes, R. L.; Wang, K. K. W.; Robertson, C. S. Original Articles GFAP Out-Performs S100 b in Detecting Traumatic Intracranial Lesions on Computed Tomography in Trauma Patients with Mild Traumatic Brain Injury and Those with Extracranial Lesions. **2014**, *1822*, 1815–1822. <https://doi.org/10.1089/neu.2013.3245>.
- (97) Posti, J. P.; Takala, R. S. K.; Runtti, H.; Newcombe, V. F.; Outtrim, J.; Katila, A. J.; Frantze, J.; Ala-seppa, H.; Coles, J. P.; Kyllö, A.; Maanpa, H.; Tallus, J.; Hutchinson, P. J.; Gils, M. Van; Menon, D. K.; Tenovuo, O.; Trauma, B.; Uni-, T.; Medicine, C.; Management, P.; Neurosciences, C.; Unit, N.; Kingdom, U.; Posti, J. P.; Online, P. The Levels of Glial Fibrillary Acidic Protein and Ubiquitin C-Terminal Hydrolase-L1 During the First Week After a Traumatic Brain Injury: Correlations With Clinical and Imaging Findings. **2016**, *79* (3), 456–464.
<https://doi.org/10.1227/NEU.0000000000001226>.

- (98) Mondello, S.; Akinyi, L.; Buki, A.; Robicsek, S.; Gabrielli, A.; Tepas, J.; Papa, L.; Brophy, G. M.; Tortella, F.; Hayes, R. L.; Wang, K. K. NIH Public Access. **2013**, *70* (3), 666–675. <https://doi.org/10.1227/NEU.0b013e318236a809.CLINICAL>.
- (99) EVALUATION OF AUTOMATIC CLASS III DESIGNATION FOR Banyan Brain Trauma Indicator. No. 82, 1–32.
- (100) Zetterberg, H.; Smith, D. H.; Blennow, K. Biomarkers of Mild Traumatic Brain Injury in Cerebrospinal Fluid and Blood. *Nat. Rev. Neurol.* **2013**, *9* (4), 201–210. <https://doi.org/10.1038/nrneurol.2013.9>.
- (101) Shahim, P.; Tegner, Y.; Wilson, D. H.; Randall, J.; Skillbäck, T.; Pazooki, D.; Kallberg, B.; Blennow, K.; Zetterberg, H. Blood Biomarkers for Brain Injury in Concussed Professional Ice Hockey Players. *JAMA Neurol.* **2014**, *71* (6), 684–692. <https://doi.org/10.1001/jamaneurol.2014.367>.
- (102) Nam, J.; Rissland, O. S.; Koppstein, D.; Abreu-goodger, C.; Jan, C. H.; Agarwal, V.; Yildirim, M. A.; Rodriguez, A.; Bartel, D. P. Nihms-577451. **2015**, *53* (6), 1031–1043. <https://doi.org/10.1016/j.molcel.2014.02.013.Global>.
- (103) Atif, H.; Hicks, S. D. A Review of MicroRNA Biomarkers in Traumatic Brain Injury. *J. Exp. Neurosci.* **2019**, *13*, 117906951983228. <https://doi.org/10.1177/1179069519832286>.
- (104) Yang, T.; Song, J.; Bu, X.; Wang, C.; Wu, J.; Cai, J.; Wan, S.; Fan, C.; Zhang, C.; Wang, J. Elevated Serum MiR-93, MiR-191, and MiR-499 Are Noninvasive Biomarkers for the Presence and Progression of Traumatic Brain Injury. *J. Neurochem.* **2016**, *137* (1), 122–129. <https://doi.org/10.1111/jnc.13534>.
- (105) Redell, J. B.; Moore, A. N.; Ward, N. H.; Hergenroeder, G. W.; Dash, P. K. Human Traumatic Brain Injury Alters Plasma Microrna Levels. *J. Neurotrauma* **2010**, *27* (12), 2147–2156. <https://doi.org/10.1089/neu.2010.1481>.
- (106) Di Pietro, V.; Porto, E.; Ragusa, M.; Barbagallo, C.; Davies, D.; Forcione, M.; Logan, A.; Di Pietro, C.; Purrello, M.; Grey, M.; Hammond, D.; Sawlani, V.; Barbey, A. K.; Belli, A. Salivary MicroRNAs: Diagnostic Markers of Mild Traumatic Brain Injury in Contact-Sport. *Front. Mol. Neurosci.* **2018**, *11* (August), 1–13. <https://doi.org/10.3389/fnmol.2018.00290>.
- (107) Joglekar, M. V.; Patil, D.; Joglekar, V. M.; Rao, G. V.; Reddy, D. N.; Mitnala, S.; Shouche, Y.; Hardikar, A. A. The MiR-30 Family MicroRNAs Confer Epithelial Phenotype to Human Pancreatic Cells. *Islets* **2009**, *1* (2), 137–147. <https://doi.org/10.4161/isl.1.2.9578>.
- (108) Bou Khalil, M.; Hou, W.; Zhou, H.; Elisma, F.; Swayne, L. A.; Blanchard, A. P.; Yao, Z.; Bennett, S. A. L.; Figeys, D. Lipidomics Era: Accomplishments and Challenges. *Mass Spectrom. Rev.* **2010**, *29* (6), 877–929. <https://doi.org/10.1002/mas.20294>.
- (109) Piomelli, D.; Astarita, G.; Rapaka, R. A Neuroscientist’s Guide to Lipidomics. *Nat. Rev. Neurosci.* **2007**, *8* (10), 743–754. <https://doi.org/10.1038/nrn2233>.
- (110) Kay, A. D.; Day, S. P.; Kerr, M.; Nicoll, J. A. R.; Packard, C. J.; Caslake, M. J. Remodeling of Cerebrospinal Fluid Lipoprotein Particles after Human Traumatic Brain Injury. *J. Neurotrauma* **2003**, *20* (8), 717–723. <https://doi.org/10.1089/089771503767869953>.
- (111) Hogan, S. R.; Phan, J. H.; Alvarado-Velez, M.; Wang, M. D.; Bellamkonda, R. V.; Fernández, F. M.; LaPlaca, M. C. Discovery of Lipidome Alterations Following

- Traumatic Brain Injury via High-Resolution Metabolomics. *J. Proteome Res.* **2018**, *17* (6), 2131–2143. <https://doi.org/10.1021/acs.jproteome.8b00068>.
- (112) Nessel, I.; Michael-Titus, A. T. Lipid Profiling of Brain Tissue and Blood after Traumatic Brain Injury: A Review of Human and Experimental Studies. *Semin. Cell Dev. Biol.* **2020**. <https://doi.org/10.1016/j.semcdb.2020.08.004>.
- (113) Colas, R. A.; Shinohara, M.; Dalli, J.; Chiang, N.; Serhan, C. N. Identification and Signature Profiles for Pro-Resolving and Inflammatory Lipid Mediators in Human Tissue. *Am. J. Physiol. - Cell Physiol.* **2014**, *307* (1), 39–54. <https://doi.org/10.1152/ajpcell.00024.2014>.
- (114) Dennis, E. A.; Norris, P. C. Eicosanoid Storm in Infection and Inflammation. *Nat. Rev. Immunol.* **2015**, *15* (8), 511–523. <https://doi.org/10.1038/nri3859>.
- (115) Pilitsis, J. G.; Coplin, W. M.; O'Regan, M. H.; Wellwood, J. M.; Diaz, F. G.; Fairfax, M. R.; Michael, D. B.; Phillis, J. W. Free Fatty Acids in Cerebrospinal Fluids from Patients with Traumatic Brain Injury. *Neurosci. Lett.* **2003**, *349* (2), 136–138. [https://doi.org/10.1016/S0304-3940\(03\)00803-6](https://doi.org/10.1016/S0304-3940(03)00803-6).
- (116) Pilitsis, J. G.; Coplin, W. M.; O'Regan, M. H.; Wellwood, J. M.; Diaz, F. G.; Fairfax, M. R.; Michael, D. B.; Phillis, J. W. Free Fatty Acids in Human Cerebrospinal Fluid Following Subarachnoid Hemorrhage and Their Potential Role in Vasospasm: A Preliminary Observation. *J. Neurosurg.* **2002**, *97* (2), 272–279. <https://doi.org/10.3171/jns.2002.97.2.0272>.
- (117) Olsson, N. U.; Harding, A. J.; Harper, C.; Salem, N. High-Performance Liquid Chromatography Method with Light-Scattering Detection for Measurements of Lipid Class Composition: Analysis of Brains from Alcoholics. *J. Chromatogr. B Biomed. Appl.* **1996**, *681* (2), 213–218. [https://doi.org/10.1016/0378-4347\(95\)00576-5](https://doi.org/10.1016/0378-4347(95)00576-5).
- (118) Pasvogel, A. E.; Miketova, P.; Moore, I. M. (Ki). Cerebrospinal Fluid Phospholipid Changes Following Traumatic Brain Injury. *Biol. Res. Nurs.* **2008**, *10* (2), 113–120. <https://doi.org/10.1177/1099800408323218>.
- (119) Pasvogel, A. E.; Miketova, P.; Moore, I. M. Differences in CSF Phospholipid Concentration by Traumatic Brain Injury Outcome. *Biol. Res. Nurs.* **2010**, *11* (4), 325–331. <https://doi.org/10.1177/1099800409346056>.
- (120) Emmerich, T.; Abdullah, L.; Crynen, G.; Dretsch, M.; Evans, J.; Ait-Ghezala, G.; Reed, J.; Montague, H.; Chaytow, H.; Mathura, V.; Martin, J.; Pelot, R.; Ferguson, S.; Bishop, A.; Phillips, J.; Mullan, M.; Crawford, F. Plasma Lipidomic Profiling in a Military Population of Mild Traumatic Brain Injury and Post-Traumatic Stress Disorder with Apolipoprotein e E4-Dependent Effect. *J. Neurotrauma* **2016**, *33* (14), 1331–1348. <https://doi.org/10.1089/neu.2015.4061>.
- (121) Choi, J. W.; Chun, J. Lysophospholipids and Their Receptors in the Central Nervous System. *Biochim. Biophys. Acta - Mol. Cell Biol. Lipids* **2013**, *1831* (1), 20–32. <https://doi.org/10.1016/j.bbalip.2012.07.015>.
- (122) Ogasawara, D.; Deng, H.; Viader, A.; Baggelaar, M. P.; Breman, A.; den Dulk, H.; van den Nieuwendijk, A. M. C. H.; Soethoudt, M.; van der Wel, T.; Zhou, J.; Overkleeft, H. S.; Sanchez-Alavez, M.; Mori, S.; Nguyen, W.; Conti, B.; Liu, X.; Chen, Y.; Liu, Q.; Cravatt, B. F.; van der Stelt, M. Rapid and Profound Rewiring of Brain Lipid Signaling Networks by Acute Diacylglycerol Lipase Inhibition. *Proc. Natl. Acad. Sci.* **2016**, *113* (1), 26–33.

- <https://doi.org/10.1073/pnas.1522364112>.
- (123) Ji, J.; Kline, A. E.; Amoscato, A.; Samhan-Arias, A. K.; Sparvero, L. J.; Tyurin, V. A.; Tyurina, Y. Y.; Fink, B.; Manole, M. D.; Puccio, A. M.; Okonkwo, D. O.; Cheng, J. P.; Alexander, H.; Clark, R. S. B.; Kochanek, P. M.; Wipf, P.; Kagan, V. E.; Bayir, H. Lipidomics Identifies Cardiolipin Oxidation as a Mitochondrial Target for Redox Therapy of Brain Injury. *Nat. Neurosci.* **2012**, *15* (10), 1407–1413. <https://doi.org/10.1038/nn.3195>.
- (124) Schrimpe-Rutledge, A. C.; Codreanu, S. G.; Sherrod, S. D.; McLean, J. A. Untargeted Metabolomics Strategies—Challenges and Emerging Directions. *J. Am. Soc. Mass Spectrom.* **2016**, *27* (12), 1897–1905. <https://doi.org/10.1007/s13361-016-1469-y>.
- (125) Johnson, C. H.; Gonzalez, F. J. Challenges and Opportunities of Metabolomics. *J. Cell. Physiol.* **2012**, *227* (8), 2975–2981. <https://doi.org/10.1002/jcp.24002>.
- (126) Luffer-Atlas, D. Unique/Major Human Metabolites: Why, How, and When to Test for Safety in Animals. *Drug Metab. Rev.* **2008**, *40* (3), 447–463. <https://doi.org/10.1080/03602530802186561>.
- (127) Vinayavekhin, N.; Saghatelian, A. Untargeted Metabolomics. In *Current Protocols in Molecular Biology*; John Wiley & Sons, Inc.: Hoboken, NJ, USA, 2010. <https://doi.org/10.1002/0471142727.mb3001s90>.
- (128) Roberts, L. D.; Souza, A. L.; Gerszten, R. E.; Clish, C. B. *Targeted Metabolomics NIH Public Access*; 2012. <https://doi.org/10.1002/0471142727.mb3002s98.Targeted>.
- (129) Wenk, M. R. Lipidomics: New Tools and Applications. *Cell* **2010**, *143* (6), 888–895. <https://doi.org/10.1016/j.cell.2010.11.033>.
- (130) Bedair, M.; Sumner, L. W. Current and Emerging Mass-Spectrometry Technologies for Metabolomics. *TrAC - Trends Anal. Chem.* **2008**, *27* (3), 238–250. <https://doi.org/10.1016/j.trac.2008.01.006>.
- (131) El-Aneed, A.; Cohen, A.; Banoub, J. Mass Spectrometry, Review of the Basics: Electrospray, MALDI, and Commonly Used Mass Analyzers. *Appl. Spectrosc. Rev.* **2009**, *44* (3), 210–230. <https://doi.org/10.1080/05704920902717872>.
- (132) Martin, A.; Smart, J. Gas-Phase Chromatography. *Nature* **1955**, *17* (2), 422–423.
- (133) Jandera, P. LIQUID Chromatography | Normal Phase. *Encycl. Anal. Sci.* **2005**, 162–173. <https://doi.org/10.1016/B978-0-12-409547-2.00300-0>.
- (134) Pham, T. H.; Zaeem, M.; Fillier, T. A.; Nadeem, M.; Vidal, N. P.; Manful, C.; Cheema, S.; Cheema, M.; Thomas, R. H. Targeting Modified Lipids during Routine Lipidomics Analysis Using HILIC and C30 Reverse Phase Liquid Chromatography Coupled to Mass Spectrometry. *Sci. Rep.* **2019**, *9* (1), 1–15. <https://doi.org/10.1038/s41598-019-41556-9>.
- (135) Hilaire, P. B. Saint; Rousseau, K.; Seyer, A.; Dechaumet, S.; Damont, A.; Junot, C.; Fenaille, F. Comparative Evaluation of Data Dependent and Data Independent Acquisition Workflows Implemented on an Orbitrap Fusion for Untargeted Metabolomics. *Metabolites* **2020**, *10* (4). <https://doi.org/10.3390/metabo10040158>.
- (136) Fenaille, F.; Barbier Saint-Hilaire, P.; Rousseau, K.; Junot, C. Data Acquisition Workflows in Liquid Chromatography Coupled to High Resolution Mass Spectrometry-Based Metabolomics: Where Do We Stand? *J. Chromatogr. A* **2017**, *1526* (March), 1–12. <https://doi.org/10.1016/j.chroma.2017.10.043>.

- (137) Spengler, B.; Hubert, M.; Kaufman, R. MALDI Ion Imaging and Biological Ion Imaging with a New Scanning UV-Laser Microprobe. 42 Annual Conf. On Mass Spectrom. and Allied Topics ASMS: Chicago, IL 1994, p 1.
- (138) Caprioli, R. M.; Farmer, T. B.; Gile, J. Molecular Imaging of Biological Samples : Localization of Peptides and Proteins Using MALDI-TOF MS. **1997**, *69* (23), 4751–4760. <https://doi.org/10.1021/ac970888i>.
- (139) Suder, A. B.-K. and P. Imaging Mass Spectrometry: Instrumentation, Applications, and Combination with Other Visualization Techniques. *Mass Spectrom. Rev.* **2016**, *35*, 147–169. <https://doi.org/10.1002/mas>.
- (140) Takáts, Z.; Wiseman, J. M.; Gologan, B.; Cooks, R. G. Mass Spectrometry Sampling under Ambient Conditions with Desorption Electrospray Ionization. *Science* (80-.). **2004**, *306* (5695), 471–473. <https://doi.org/10.1126/science.1104404>.
- (141) Wiseman, J. M.; Cooks, R. G. SPECIAL FEATURE : Ambient Mass Spectrometry Using Desorption Electrospray Ionization (DESI): Instrumentation , Mechanisms and Applications in Forensics , Chemistry ,. *J. Mass Spectrom.* **2005**, No. 40, 1261–1275. <https://doi.org/10.1002/jms.922>.
- (142) Bingol, K. Recent Advances in Targeted and Untargeted Metabolomics by NMR and MS/NMR Methods. *High-Throughput* **2018**, *7* (2). <https://doi.org/10.3390/ht7020009>.
- (143) Markley, J. L.; Brüschweiler, R.; Edison, A. S.; Eghbalian, H. R.; Powers, R.; Raftery, D.; Wishart, D. S. The Future of NMR-Based Metabolomics. *Curr. Opin. Biotechnol.* **2017**, *43*, 34–40. <https://doi.org/10.1016/j.copbio.2016.08.001>.
- (144) Emwas, A. H.; Roy, R.; McKay, R. T.; Tenori, L.; Saccenti, E.; Nagana Gowda, G. A.; Raftery, D.; Alahmari, F.; Jaremko, L.; Jaremko, M.; Wishart, D. S. Nmr Spectroscopy for Metabolomics Research. *Metabolites* **2019**, *9* (7). <https://doi.org/10.3390/metabo9070123>.
- (145) Shen, X.; Gong, X.; Cai, Y.; Guo, Y.; Tu, J. Normalization and Integration of Large-Scale Metabolomics Data Using Support Vector Regression. *Metabolomics* **2016**, *12* (5), 1–12. <https://doi.org/10.1007/s11306-016-1026-5>.
- (146) Eliasson, M.; Ra, S.; Madsen, R.; Donten, M. A.; Marsden-edwards, E.; Moritz, T.; Shockcor, J. P.; Johansson, E.; Trygg, J. Strategy for Optimizing LC-MS Data Processing in Metabolomics: A Design of Experiments Approach. *Anal. Chem.* **2012**, *84* (15), 6869–6876. <https://doi.org/https://doi.org/10.1021/ac301482k>.
- (147) Ejigu, B. A.; Valkenburg, D.; Baggerman, G.; Vanaerschot, M.; Witters, E. Evaluation of Normalization Methods to Pave the Way Towards Large-Scale LC-MS-Based. **2013**, *17* (9). <https://doi.org/10.1089/omi.2013.0010>.
- (148) Broadhurst, D.; Goodacre, R.; Reinke, S. N.; Kuligowski, J.; Wilson, I. D.; Lewis, M. R.; Dunn, W. B. Guidelines and Considerations for the Use of System Suitability and Quality Control Samples in Mass Spectrometry Assays Applied in Untargeted Clinical Metabolomic Studies. *Metabolomics* **2018**, *14* (6), 1–17. <https://doi.org/10.1007/s11306-018-1367-3>.
- (149) Worley, B.; Powers, R. Multivariate Analysis in Metabolomics. *Curr Metabolomics* **2015**, *1* (1), 92–107. <https://doi.org/10.2174/2213235X11301010092.Multivariate>.
- (150) van den Berg, R. A.; Hoefsloot, H. C. J.; Westerhuis, J. A.; Smilde, A. K.; van der

- Werf, M. J. Centering, Scaling, and Transformations: Improving the Biological Information Content of Metabolomics Data. *BMC Genomics* **2006**, *7*, 1–15. <https://doi.org/10.1186/1471-2164-7-142>.
- (151) Szymanska, E.; Saccenti, E.; Smilde, A.; Westerhuis, J. Double-Check: Validation of Diagnostic Statistics for PLS-DA Models in Metabolomics Studies. *Metabolomics* **2012**, *8*, 3–16.
- (152) Leardi, R.; Gonzalez, A. Genetic Algorithms Applied to Feature Selection in PLS Regression : How and When to Use Them. *Chemom. Intell. Lab. Syst.* **1998**, *41*, 195–207.
- (153) Cai, Q.; Alvarez, J. A.; Kang, J.; Yu, T. Network Marker Selection for Untargeted LC – MS Metabolomics Data. *J. Proteome Res.* **2017**, *16* (3), 1261–1269. <https://doi.org/10.1021/acs.jproteome.6b00861>.
- (154) Rubingh, C. M.; Bijlsma, S.; Derks, E. P. P. A.; Bobeldijk, I.; Verheij, E. R.; Kochhar, S.; Smilde, A. K. Assessing the Performance of Statistical Validation Tools for Megavariate Metabolomics Data. *Metabolomics* **2006**, *2* (2), 53–61. <https://doi.org/10.1007/s11306-006-0022-6>.
- (155) Antignac, J. P.; De Wasch, K.; Monteau, F.; De Brabander, H.; Andre, F.; Le Bizec, B. The Ion Suppression Phenomenon in Liquid Chromatography-Mass Spectrometry and Its Consequences in the Field of Residue Analysis. *Anal. Chim. Acta* **2005**, *529* (1-2 SPEC. ISS.), 129–136. <https://doi.org/10.1016/j.aca.2004.08.055>.
- (156) Thissen, D.; Steinberg, L.; Kuang, D. Quick and Easy Implementation of the Benjamini-Hochberg Procedure for Controlling the False Positive Rate in Multiple Comparisons. *J. Educ. Behav. Stat.* **2002**, *27* (1), 77–83. <https://doi.org/10.3102/10769986027001077>.
- (157) Zimmerman, D. W.; Zumbo, B. D. Rank Transformations and the Power of the Student t Test and Welch t' Test for Non-Normal Populations with Unequal Variances. *Can. J. Exp. Psychol. Can. Psychol. expérimentale* **1993**, *47* (3), 523–539. <https://doi.org/10.1037/h0078850>.
- (158) Sipper, M. Evolutionary Computation in Medicine. **2000**, *19*, 1–23.
- (159) Zou, W.; Tolstikov, V. V. Pattern Recognition and Pathway Analysis with Genetic Algorithms in Mass Spectrometry Based Metabolomics. *Algorithms* **2009**, *2* (2), 638–666. <https://doi.org/10.3390/a2020638>.
- (160) Ojala, M.; Garriga, G. C. Permutation Tests for Studying Classifier Performance. *J. Mach. Learn. Res.* **2010**, *11*, 1833–1863.
- (161) Fahy, E.; Sud, M.; Cotter, D.; Subramaniam, S. LIPID MAPS Online Tools for Lipid Research. *Nucleic Acids Res.* **2007**, *35* (SUPPL.2), 606–612. <https://doi.org/10.1093/nar/gkm324>.
- (162) Fahy, E.; Subramaniam, S.; Murphy, R. C.; Nishijima, M.; Raetz, C. R. H.; Shimizu, T.; Spener, F.; Van Meer, G.; Wakelam, M. J. O.; Dennis, E. A. Update of the LIPID MAPS Comprehensive Classification System for Lipids. *J. Lipid Res.* **2009**, *50* (SUPPL.), 9–14. <https://doi.org/10.1194/jlr.R800095-JLR200>.
- (163) Guijas, C.; Montenegro-Burke, J. R.; Domingo-Almenara, X.; Palermo, A.; Warth, B.; Hermann, G.; Koellensperger, G.; Huan, T.; Uritboonthai, W.; Aisporna, A. E.; Wolan, D. W.; Spilker, M. E.; Benton, H. P.; Siuzdak, G. METLIN: A Technology Platform for Identifying Knowns and Unknowns. *Anal. Chem.* **2018**, *90* (5), 3156–

3164. <https://doi.org/10.1021/acs.analchem.7b04424>.
- (164) Wishart, D. S.; Feunang, Y. D.; Marcu, A.; Guo, A. C.; Liang, K.; Vázquez-Fresno, R.; Sajed, T.; Johnson, D.; Li, C.; Karu, N.; Sayeeda, Z.; Lo, E.; Assempour, N.; Berjanskii, M.; Singhal, S.; Arndt, D.; Liang, Y.; Badran, H.; Grant, J.; Serra-Cayuela, A.; Liu, Y.; Mandal, R.; Neveu, V.; Pon, A.; Knox, C.; Wilson, M.; Manach, C.; Scalbert, A. HMDB 4.0: The Human Metabolome Database for 2018. *Nucleic Acids Res.* **2018**, *46* (D1), D608–D617. <https://doi.org/10.1093/nar/gkx1089>.
- (165) Ojo, J. O.; Algamal, M.; Leary, P.; Abdullah, L.; Mouzon, B.; Evans, J. E.; Mullan, M.; Crawford, F. Disruption in Brain Phospholipid Content in a Humanized Tau Transgenic Model Following Repetitive Mild Traumatic Brain Injury. *Front. Neurosci.* **2018**, *12* (December), 1–18. <https://doi.org/10.3389/fnins.2018.00893>.
- (166) Srivastava, N. K.; Mukherjee, S.; Sharma, R.; Das, J.; Sharma, R.; Kumar, V.; Sinha, N.; Sharma, D. Altered Lipid Metabolism in Post-Traumatic Epileptic Rat Model: One Proposed Pathway. *Mol. Biol. Rep.* **2019**, *46* (2), 1757–1773. <https://doi.org/10.1007/s11033-019-04626-9>.
- (167) Barbacci, D. C.; Roux, A.; Muller, L.; Jackson, S. N.; Post, J.; Baldwin, K.; Ho, B.; Balaban, C. D.; Schultz, J. A.; Gouty, S.; Cox, B. M.; Woods, A. S. Mass Spectrometric Imaging of Ceramide Biomarkers Tracks Therapeutic Response in Traumatic Brain Injury. **2017**, 2266–2274. <https://doi.org/10.1021/acschemneuro.7b00189>.
- (168) Roux, A.; Muller, L.; Jackson, S. N.; Post, J.; Baldwin, K.; Hoffer, B.; Balaban, C. D.; Barbacci, D.; Schultz, J. A.; Gouty, S.; Cox, B. M.; Woods, A. S. Mass Spectrometry Imaging of Rat Brain Lipid Profile Changes over Time Following Traumatic Brain Injury. *J. Neurosci. Methods* **2016**, *272*, 19–32. <https://doi.org/10.1016/j.jneumeth.2016.02.004>.
- (169) Novgorodov, S. A.; Riley, C. L.; Yu, J.; Borg, K. T.; Hannun, Y. A.; Proia, R. L.; Kindy, M. S.; Gudz, T. I. Essential Roles of Neutral Ceramidase and Sphingosine in Mitochondrial Dysfunction Due to Traumatic Brain Injury. *J. Biol. Chem.* **2014**, *289* (19), 13142–13154. <https://doi.org/10.1074/jbc.M113.530311>.